1994). Many food- or water-borne diseases caused by *V. parahaemolyticus* (Sanyal and Sen 1974; Centers for Disease Control and Prevention 1998, 1999; Daniels *et al.* 2000) and *Vibrio cholerae* (Bennish 1994; Faruque *et al.* 1998) are important health problems worldwide. As these are gastrointestinal pathogens, it is implied that the pathogens successfully pass through the acidic stomach and colonize in the intestine. Waterman and Small (1998) reported that the surface-associated *V. cholerae* cells were protected from acidic environments. According to the report, *V. cholerae* cells cultured alone decreased over 5-log units in pH 5·0 Luria-Bertani (LB) medium, but in contrast, decreased only 3-log units even at pH 2·5 when inoculated with ground beef. As not all cases are transmitted by food, it is speculated that there is another factor participating in the acid resistance of Vibrionaceae. Merrell and Camilli (1999) reported that *V. cholerae* cells exposed to mildly acidic conditions (pH 5·7) survived lethal acid challenge (pH 4·5). Rhee *et al.* (2002) showed similar results in *Vibrio vulnificus*: their survival under acidic conditions was dependent on the lysine decarboxylase pathway. Although induced transcription of lysine decarboxylase genes under acidic pH is well described, the nature of transcription, particularly regarding the expression level of the genes, is not fully understood.

Wong *et al.* (1998) showed a similar result following mild acid exposure of *V. parahaemolyticus*. However, the detailed mechanism of acid resistance of *V. parahaemolyticus* remained unknown. The phenomenon of mild acid exposure enhancing the ability of the pathogens to survive under lethal acidic conditions is now referred to as acid tolerance response (ATR). ATR was first recognized in *Salmonella typhimurium* by Foster and Hall (1990), and is now recognized by several researchers as the mechanism by which bacteria break through the gastric acid barrier (Foster 1999; Audia *et al.* 2001). ATR and its correlation with infectivity have also been reported elsewhere (Wilmes-Riesenberg *et al.* 1996; Merrell and Camilli 1999). *Vibrio parahaemolyticus*, an acid-sensitive gastric pathogen, may also utilize ATR in its mode of infection. In Japan, mildly acidic sushi (vinegar is usually added to the rice, pH 4·3–4·9) is frequently implicated in outbreaks of *V. parahaemolyticus* infection (Shimada and Arakawa 2000). This problem is suggestive of the importance of ATR in *V. parahaemolyticus* infection.

In this study, we focused on the ATR of *V. parahaemolyticus* using *in vitro* acid resistance tests. Molecular analysis for the ATR-associated gene, lysine decarboxylase, was also conducted, and the transcription patterns were precisely demonstrated by SYBR Green I real-time reverse transcriptional (RT) polymerase chain reaction (PCR) and Northern blot hybridization. Finally, a lysine decarboxylase gene-inactivated strain was constructed to clarify the role of this enzyme in ATR.

Materials and methods

Bacterial strains and growth conditions

A total of 11 *V. parahaemolyticus* strains, VpTK-(1, 3, 6, 8, 9, 10, 11, 12, 13, 17) and strain V02-64, representing the newly emerged clone of serotype O3:K6, were used. All *V. parahaemolyticus* strains (*tdh*+, Kanagawa phenomenon positive) isolated from food-poisoning patients were stored at −80°C using MicroBank microbial storage kits (Pro-Lab Diagnostics, Ontario, Canada) until use. All strains were serotyped by the slide agglutination test with O- and K-antigens using commercially available antisera (*V. parahaemolyticus* antisera Seiken set, Denka Seiken, Tokyo, Japan). Unless otherwise noted, all *V. parahaemolyticus* strains were cultured in LB broth or on LB agar (1·5% agar) with 3% sodium chloride. *Escherichia coli* strain JM109 used for genetic manipulation was grown in LB broth or on LB agar supplemented with 5 μg ml^{-1} ampicillin unless otherwise specified.

Adaptive acid tolerance assays

Overnight cultures (300 μl) of each *V. parahaemolyticus* strain were inoculated into 30 ml fresh LB broth and incubated at 30°C with shaking until the OD_{600} reached 0·16–0·20 (log-phase culture). An aliquot of this culture (1 ml) was harvested by centrifugation at 15 000 *g* for 3 min at room temperature. Cells were resuspended in 1 ml of LB-MES (100 mmol l^{-1} 4-morpholinoethanesulfonic acid (MES), pH 5·5) or LB-HEPES (100 mmol l^{-1} [4-(2-hydroxyethyl)-1-piperazinyl]ethanesulfonic acid (HEPES), pH 7·5) and incubated at 37°C for 1 h. Cultures were centrifuged at 15 000 *g* for 3 min at room temperature, and the pellets were resuspended in 1 ml of LB broth (pH 4·0) and incubated at 37°C for 1 h. Immediately after resuspension in LB broth (pH 4·0), portions of samples were serially diluted in phosphate-buffered saline (PBS) (pH 7·0) and plated onto trypticase soy agar (TSA; Difco Laboratories, Detroit, MI, USA) with a spiral plater (IUL Instruments, Barcelona, Spain) (initial count). After 1 h of incubation in LB broth (pH 4·0), viable cells were enumerated in the same fashion (survival count), and the per cent surviving the acid challenge was calculated by dividing the viable counts at 1 h by the initial viable counts and multiplying by 100. The amount of some polyamines (tryptamine, putrescine, cadaverine, histamine, agmatine, tyramine, and spermidine) in the LB broth was measured by HPLC as previously described (Yamanaka and Matsumoto 1989).

Lysine decarboxylase-dependent acid-tolerance assays

Overnight cultures (500 μl) of each *V. parahaemolyticus* strain were inoculated into 50 ml fresh LB broth (1 : 100) and incubated at 30°C with shaking (170 rev min^{-1}) until OD_{600} reached 0·16–0·20 (log-phase culture). Cells were precipitated and resuspended in LB-MES, pH 5·5 (acid adaptation) or LB-HEPES, pH 7·5 (no adaptation). Chloramphenicol was added at 10 μg ml^{-1} to each treatment in order to assay the ATR in the absence of *de novo* protein synthesis during acid adaptation. After incubation for 1 h, cells were washed twice with no citrate E medium (NCE; Maloy and Roth 1983) at pH 5·5 or 7·5 (pH adjusted with HCl) and resuspended in equal volumes of NCE, pH 4·0 (acid challenge) with or without 1% L-lysine hydrochloride. Viable counts were performed immediately after resuspension in NCE and at subsequent 30-min intervals.

DNA manipulation and sequencing

Chromosomal DNA of *V. parahaemolyticus* was isolated according to the standard protocol (Sambrook *et al.* 1989) and plasmid DNA was purified using Quantum prep plasmid miniprep kits (Bio-Rad Laboratories, Richmond, CA, USA). A degenerate primer pair, 5′-GTN CTW TAY TAY CAC GCN AAC TGG A-3′ and 5′-GCY TSN CRN ACC ARC ATC ATC CA-3′, for lysine/cadaverine antiporter (*cadB*) was designed from other known CadB amino acid sequences: *E. coli* (sequence accession number: NC000913), *Salmonella typhimurium* (AE008816), *V. cholerae* (NC002505), and *V. vulnificus* (AF324470). After amplifying the homologous *V. parahaemolyticus cadB* fragment using this primer pair at an annealing temperature of 58°C, the PCR products were cloned into pT7-Blue T-vector (Novagen, Madison, WI, USA) and the sequences of several clones were determined.

Unidentified regions around *cadB* were amplified and cloned using partial sequence information and LA (long and accurate) PCR *in vitro* cloning kits (Takara Bio, Shiga, Japan), according to the manufacturer's instructions. Briefly, chromosomal DNA digested with the appropriate restriction enzymes and adapters (double-stranded oligonucleotides) were ligated. Then, the fragments containing unknown regions were amplified using an adapter primer and a primer specific to the partial *cadB* sequence. The resulting products were cloned into pT7Blue T-vectors (all restriction enzymes and DNA ligase were provided by Takara Bio). Several clones were sequenced using BigDye terminator cycle sequencing kits (Applied Biosystems, Foster City, CA, USA) and analysed on an ABI310 genetic analyser (Applied Biosystems). Sequences were assembled and analysed by GENETYX-MAC software (Software Development Co., Ltd, Tokyo, Japan).

RNA extraction and Northern blot hybridization

Log-phase cultures (45 ml) were pelleted and resuspended in 45 ml of LB-MES (pH 5·5) or LB-HEPES (pH 7·5). After 2 h of incubation at 30°C, total RNA was isolated using TRIzol reagent (Invitrogen, Carlsbad, CA, USA) according to the manufacturer's instructions, followed by DNase I (RNase free, Wako Pure Chemical Industries, Japan) treatment for 30 min. Blotting of total RNA was performed as follows: 15 μg of total RNA was loaded onto 1% Seakem GTG (FMC BioProducts, Rockland, ME, USA) agarose gels, electrophoresed in MOPS buffer (0·4 mol l^{-1} 3-morpholinopropanesulfonic acid (MOPS), 0·1 mol l^{-1} sodium acetate, 15 mmol l^{-1} EDTA, pH 7·0) with size markers for RNA (Perfect RNA markers, 0·2–10 kb; Novagen), and blotted to Hybond-N+ membranes (Amersham Biosciences Corp., Piscataway, NJ, USA) with an electroblotter, NB-1513 (Nihon Eidoh, Tokyo, Japan). Hybridization was done with ECL (enhanced chemical luminescence) direct nucleic acid labelling kit (Amersham Biosciences) using DNA probes specific for *cadA* or *cadB*, prepared by PCR using primers 5′-TTA TCA CGC CAA CTG GAT TGG-3′ and 5′-GCG TGT AGC TTC ATG TAC TGA GC-3′ for *cadB*, and 5′-CCT CCA TTC AAC TAA AGC GCT A-3′ and 5′-CAA TGC CGT ACT GAG GTG AAG-3′ for *cadA*.

RT-PCR for mRNA quantification

In SYBR Green I real-time quantitative PCR, amplification of cDNA is measured by the increase in fluorescence resulting from the successive intercalation of SYBR Green I dye into the double-stranded DNA. The threshold cycle (*Ct*), the first PCR cycle in which the incremental increase in fluorescence can be detected, is used to calculate the initial amount of template DNA based on a standard curve plot of cDNA derived from the *Ct* values calculated from known concentrations of the standard DNA. Moreover, the specificity of all PCR reactions were verified based on the melting temperature (T_m) measured by the 'disassociation curve' analysis on an ABI 7900HT (Applied Biosystems) immediately after amplification. T_m is unique to the amplification products and is determined by the decrease in fluorescence from SYBR Green I dye during slow heating (from 60 to 95°C). Data collection and multicomponent analyses were performed with the Sequence Detection Software 2·0 supplied with ABI prism 7900HT (Applied Biosystems). An endogenous control of sample RNA, 16S rRNA, was also quantified and used for data analyses.

Primer selection

A total of four amplifications were designed to study the transcription of *cadBA* genes of *V. parahaemolyticus*. The *cadB* mRNA (519 bp) was amplified by primers 5′-ATT CGG TAG CTG GAC TGC AC-3′ and 5′-GCG TGT AGC TTC ATG TAC TGA GC-3′ and *cadA* mRNA (443 bp) was amplified by primers 5′-GTA TTC TTC CCT GTG CTT AAT GAC-3′ and 5′-GCA GTC ACA ATC GCA TGG CTA TCA-3′. The *cadBA* bi-cistronic mRNA (403 bp) was amplified by primers 5′-GCT TCG TAA TGC TGT TCT CTG G-3′ and 5′-CGT AGC CCG CTT TCT CAA GA-3′, which were designed to target the C-termini of *cadB* and the *N*-termini of *cadA*. The precise primer locations are shown in Fig. 2. Universal primers 510f and 920r were used to amplify 16S rRNA for endogenous reference. Reverse transcription was performed with randomly synthesized hexanucleotide [random hexamer, $d(N)_6$; Applied Biosystems].

RT of RNA

The RT reactions were carried out with the following recipe: 5·0 mmol l^{-1} of $MgCl_2$, 2·0 mmol l^{-1} of each dNTP, 2·5 μmol l^{-1} of $d(N)_6$, 0·4 U μl^{-1} of RNase Inhibitor, 1·25 U μl^{-1} of MultiScribe RTase, 200 ng of total RNA, and reacted in the supplied 10 × RT buffer at 1 × concentration. All reagents were purchased from Applied Biosystems. RNA samples extracted from each type of cells were purified by treatment with DNase I for the removal of residual DNA contamination. RT reactions were performed in a GeneAmp 9700 (Applied Biosystems) with a thermal profile of 25°C for 10 min, 37°C for 60 min followed by 95°C for 5 min to inactivate residual RTase, and a 4°C soak. Resultant cDNA were then applied to the SYBR Green I real-time quantitative PCR after purification by ethanol precipitation as described elsewhere.

Amplification

SYBR Green I real-time PCR was performed on an ABI prism 7900HT with Sequence Detector Software 2.0 (Applied Biosystems). Thermal cycling was performed with the following protocol: 50°C for 2 min; 95°C for 10 min; 50 cycles of 95°C for 20 s, 58°C for 45 s, and 72°C for 45 s; and an extension phase for dissociation analysis of 95°C for 15 s followed by ramping from 60°C to 95°C in 30 min. During these cycles, fluorescent signals were measured at 521 nm every 7 s, and the data were analysed after all cycles and dissociation curve analyses had been finished. The 25-μl reaction mixture contained 1 × SYBR Green buffer, 3 mmol l^{-1} of $MgCl_2$, 1 mmol l^{-1} of d(ATP, CTP, GTP) and 2 mmol l^{-1} of dUTP, 0·2 μmol l^{-1} of each primer, 0·01 U μl^{-1} of uracil-*N*-glycosidase (AmpErase UNG), 0·025 U μl^{-1} of AmpliTaq Gold DNA polymerase, and 2 μl of template cDNA (or known concentration of genomic DNA) solution. All reagents except oligonucleotide primers were supplied from Applied Biosystems. All runs contained standard templates for calculating the standard curve, as well as controls with no reverse transcription and no templates. After checking the amplification specificity by disassociation curve analysis, results were subjected to data analysis as described next. All reaction mixtures were also electrophoresed on agarose gels followed by ethidium bromide staining for visualization.

Data analyses

The measured fluorescent signals were normalized against the reference dye (6-carboxy-X-rhodamine; ROX, included in the SYBR Green buffer) and were used to calculate the ΔRn using Rn^+ (normalized signal) – Rn^- (baseline *Rn* during cycles 3–15). Data were plotted as ΔRn against the PCR cycle number, with the threshold ΔRn being set at 10 times the SD of the mean baseline signal calculated for Rn^-. The obtained *Ct* values were plotted against the amount of DNA, and a standard curve was drawn using 10-fold serial dilutions of standard DNA. A unit of 1 × DNA standard was considered to contain 5 ng μl^{-1} (or 10^5 copies) of *V. parahaemolyticus* genomic DNA. The amount of mRNA was determined using this standard curve. In order to correct for the total cell number in the RNA extraction and extraction efficiency, the quantity of 16S rRNA in each sample was used for endogenous controls, assuming that the expression of 16S rRNA is constant for all cells used in this mRNA expression analysis.

Primer extension analysis

To determine the transcriptional start position of *cadB* and *cadA* genes, we performed primer extension analyses using 5′-Texas Red labelled primers 5′-GTA AAC AAA CGC AAG GCT CAG-3′ for *cadB* mRNA and 5′-TTA TCC CAG TCG AAC AGC AC-3′ for *cadA* mRNA. Aliquots of total RNA extracted from cells exposed to pH 5·0 were reverse transcribed with ReverTra Ace (Toyobo Co. Ltd, Tokyo, Japan) according to the manufacturer's instructions. To map the transcriptional start site based on the fragment size, the extension products were separated on a 6% denaturing polyacrylamide gel on the DNA sequencer SQ5500E (Hitachi Ltd, Tokyo, Japan) along with a DNA sequence ladder prepared using the Thermo Sequenase primer cycle sequencing kit (Amersham Biosciences) to synthesize the target region with the same labelled primer.

Construction of the mutant strain

The *cadA* gene-inactivated strain, which was derived from *V. parahaemolyticus* V02-64 (serotype O3:K6) was con-

structed as previously described (Xu *et al.*, 1994). Briefly, a partial fragment of the *cadA* gene of V02-64 was isolated by PCR using primers 5′-CAA TCT ACT TCC GTC CAA CTC G-3′ and 5′-CAA TGC CGT ACT GAG GTG AAG-3′. The amplified fragment was cloned into the pT7-Blue T-vector and then digested by *Bam*HI and *Pst*I. The digested fragment was subcloned into suicide vector, pKY719 (Xu *et al.* 1994), transformed into *E. coli* SM10*λpir*, and then re-introduced into *V. parahaemolyticus* cells through conjugation at 37°C overnight on LB agar. Cells were recovered by saline, plated onto thiosulfate citrate bile salts sucrose (TCBS; Eiken Chemicals Co. Ltd, Tokyo, Japan) supplemented with 10 μg ml^{-1} of chloramphenicol, and incubated overnight at 30°C. Chloramphenicol-resistant *V. parahaemolyticus* cells with *cadA* genes inactivated by plasmid integration (single crossing-over), were screened by tests including southern blot hybridization and DNA sequencing. The lack of lysine decarboxylase activity was confirmed using an indicator broth (BBL Moeller decarboxylase broth base; Becton Dickinson, NJ, USA) and HPLC measurement as described before. Tests for biochemical characteristics were performed using ID32E API (BioMerieux, Marcy l'Etoile, France). The acid survival of the mutant and wild-type strains was measured by the same methods described before.

Nucleotide sequence accession number

The nucleotide sequence reported in this paper is available in the DDBJ/EMBL/GenBank databases under accession number AB124819 (*V. parahaemolyticus* V02-64 *cadBA*).

Results

Vibrio parahaemolyticus possesses an adaptive ATR

The adaptive acid tolerance response in *V. parahaemolyticus* was examined in several strains (Table 1). In all strains, adapted cells (LB-MES, pH 5·5) showed better survival than nonadapted (LB-HEPES, pH 7·5) cells when exposed to acid (LB-MES, pH 4·0). As we have hypothesized that lysine decarboxylating activity plays a role in the ATR of *V. parahaemolyticus*, we analysed supernatants for the presence of polyamines. The HPLC findings show a large amount of cadaverine, which is generated from lysine through decarboxylation reactions, only in cells that survive lethal acidic conditions (adapted cells, data not shown). The recently emerged *V. parahaemolyticus* serotype O3:K6 was not more acid resistant than other *V. parahaemolyticus* strains used in this study.

Table 1 Effect of acid adaptation in the acid survival of *Vibrio parahaemolyticus* strains

Strain	Per cent survival* after 1 h at pH 4·0	
	Adapted†	Nonadapted
V02-64‡	$10{\cdot}1 \pm 6{\cdot}2_{AB}$§	$0{\cdot}23 \pm 0{\cdot}20$,§
VpTK01	$32{\cdot}7 \pm 3{\cdot}4_{AB}$	$0{\cdot}21 \pm 0{\cdot}09$,
VpTK03	$15{\cdot}9 \pm 3{\cdot}8_{AB}$	$0{\cdot}84 \pm 0{\cdot}14$,
VpTK06	$7{\cdot}3 \pm 5{\cdot}6_{B}$	$0{\cdot}11 \pm 0{\cdot}05$,
VpTK08	$36{\cdot}9 \pm 0{\cdot}6_{A}$	$0{\cdot}02 \pm 0{\cdot}01$,
VpTK09	$8{\cdot}3 \pm 3{\cdot}0_{B}$	ND**
VpTK10	$18{\cdot}7 \pm 4{\cdot}5_{AB}$	$0{\cdot}03 \pm 0{\cdot}02$,
VpTK11	$13{\cdot}0 \pm 0{\cdot}5_{AB}$	ND**
VpTK12	$30{\cdot}0 \pm 11{\cdot}8_{AB}$	$0{\cdot}03 \pm 0{\cdot}01$,
VpTK13	$7{\cdot}0 \pm 5{\cdot}5_{B}$	$1{\cdot}00 \pm 0{\cdot}69$,
VpTK17	$28{\cdot}4 \pm 6{\cdot}2_{AB}$	$0{\cdot}21 \pm 0{\cdot}07$,

*Values are per cent survival after the acid challenge calculated by dividing the viable counts at 1 h by the initial viable counts and multiplying by 100. Values are the means (±SE) of three independent experiments.

†Acid adaptation was performed at pH 5·5 for 1 h at 30°C.

‡Serotype O3:K6.

§Means with the same letter within a column are not significantly different (Tukey-Kramer multiple comparison test, $P < 0{\cdot}05$).

**ND, not detected.

ATR of *Vibrio parahaemolyticus* requires external lysine

To demonstrate the dependence of ATR on lysine decarboxylase in *V. parahaemolyticus*, we determined the survival of the acid-adapted cells in NCE (pH 4·0) with or without 1% L-lysine. Tolerance of *V. parahaemolyticus* V02-64 (serotype O3:K6) to pH 4·0 NCE media was greater in the lysine supplied condition, as a threefold log reduction in survival was observed in the treatment without lysine after 60 min, while the reduction was only one order of magnitude in the treatment with lysine (Fig. 1). Nonadapted cells and adapted cells under the condition in which the protein synthesis was limited by the supplementation of the chloramphenicol in adaptation media were decreased to 10^{-3} at 30 min after resuspension in pH 4·0 NCE with lysine. This experiment was also performed for the other nine strains, and similar results were obtained. The mean per cent survival for the 10 strains at 30, 60, and 90 min at pH 4·0 was 17·8, 10·5, and 5·78, respectively, for the lysine-supplied cells, and 3·49, 0·94 and, <0·01, respectively, for the lysine-free culture conditions.

Molecular analyses of cadA and cadB genes of *Vibrio parahaemolyticus*

The high homology of bacterial lysine/cadaverine antiporter (*cadB*) genes enabled us to design degenerate

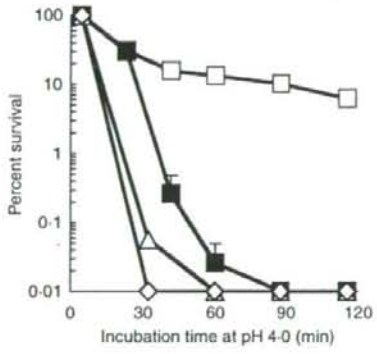

Figure 1 The fate of *Vibrio parahaemolyticus* V02-64 cells in lethally acidic environments in the presence or absence of lysine. Each cell treatment was acid adapted in Luria-Bertani (LB), pH 5·5 for 1 h and exposed to lethally acidic solution (no citrate E medium, pH 4·0) in the presence (open boxes) or absence (closed boxes) of lysine. It is notable that cells adapted with chloramphenicol (diamonds), and unadapted cells (triangles) both immediately decreased when lysine was present in the environment. All experiments were performed in triplicate, and some of the standard deviations (SD) were very small that the error bars do not extend beyond the data points.

primers based on alignments of *E. coli*, *S. typhimurium*, *V. cholerae*, and *V. vulnificus cadB* amino acid sequences. The resulting 631-bp amplification product from *V. parahaemolyticus* included six transmembrane domains as predicted by the SOSUI programme (Department of Biotechnology, Tokyo University of Agriculture and Technology; http://sosui.proteome.bio.tuat.ac.jp/sosuiframe0E.html), and was considered to be *cadB* based on high homology of the determined DNA and the deduced amino acid sequences (82% and 92%, respectively) with *V. cholerae* sequences. The periphery sequences were completely determined using a commercial kit based on the cassette ligation-mediated PCR amplification technique. Two open reading frame (ORF) sequences coded on the same strand with lengths of 2136 and 1344 bp were matched to lysine decarboxylase and lysine/cadaverine antiporter of *V. cholerae* (91·7% and 88·3%, respectively) and other bacteria in the DNA Data Bank of Japan, (http://www.ddbj.nig.ac.jp). Therefore, considering the results from the mutational study (described next) into account, we designated the two ORF as *cadA* and *cadB* (Fig. 2a). The intergenic spacer region between *cadB* and *cadA* was 116 bp (Fig. 2a). This region has inverted repeat sequences and possibly forms a stem-loop structure in mRNA and may act as a terminator of the *cadB* sole transcript. RNA transcribed from the region has an eight-base stem and a four-base loop with no mismatches. Thus, taking into account the existence of the poly-A sequence, this region is the potential terminator (Fig. 2a). Recently, the entire genomic sequence of *V. parahaemolyticus* O3:K6 strain RIMD2210633 was reported (Makino *et al.* 2003); *cad* genes had sequence identity with those reported here of 99·7% (99·8% for the amino acid sequence) for *cadB* and 100% for *cadA*. In our study, *cadA* gene function was experimentally verified using the knockout mutant (described next).

Lysine decarboxylase genes are acid-induced operon

Northern blot hybridization revealed that *cad* genes are more highly expressed under acidic conditions than under neutral conditions (Fig. 3a, pH 5·5). However, hybridization data were not informative for the effect of lysine on transcription or for operon construction. Therefore, this RNA was subjected to the RT-PCR method using $d(N)_6$ and the primers shown in Fig. 2. Significant amounts of cDNA amplification products were produced using primers specific for *cadB*, *cadA* sole transcripts, and bi-cistronic transcripts of *cadBA* (Fig. 3b), showing that transcription of *cad* genes falls into the three patterns of *cadB*, *cadA*, and *cadBA*. Based on qualitative RT-PCR of RNA extracted from acid-stressed cells, significant amounts of amplification products (*cadB*, *cadA* and *cadBA*, Fig. 3b, lanes 1–4) were produced while only *cadA* amplification products were faintly observed in non-stressed cells (Fig. 3b, lanes 5 and 6). This shows that *cadBA* genes construct an operon, and the expression of *cadB*, *cadA*, and *cadBA* mRNA, especially *cadB* and *cadA*, are acid-inducible and low levels of transcription are also present at neutral pH.

RT-PCR gives more detailed information than the Northern method, although an accurate comparison of the expression ratio between these transcripts is not possible because of the 'plateau' effect of PCR end-point analysis and the variation in PCR efficiency between the experiments. Therefore, SYBR Green I real-time, quantitative RT-PCR was also performed to determine the relative expression of these mRNA species. Relative expression ratios showed that the expression of these genes was induced under the condition of low pH (Fig. 3c). For example, *cadA* mRNA exhibited about 40-fold greater expression at pH 5·0 (3·39 ± 1·5) than at pH 5·5 (0·082 ± 0·02). In cells exposed to pH 7·5, only the *cadA* transcript was detected, and this transcript showed the largest quantity under all conditions. In addition, the amount of *cadB* and *cadA* single transcripts was nearly 10- and 100-fold higher than the polycistronic *cadBA* transcript for each pH condition (Fig. 3c). For example, at pH 5·5 with the addition of lysine, the bi-cistronic *cadBA* transcript had a relative

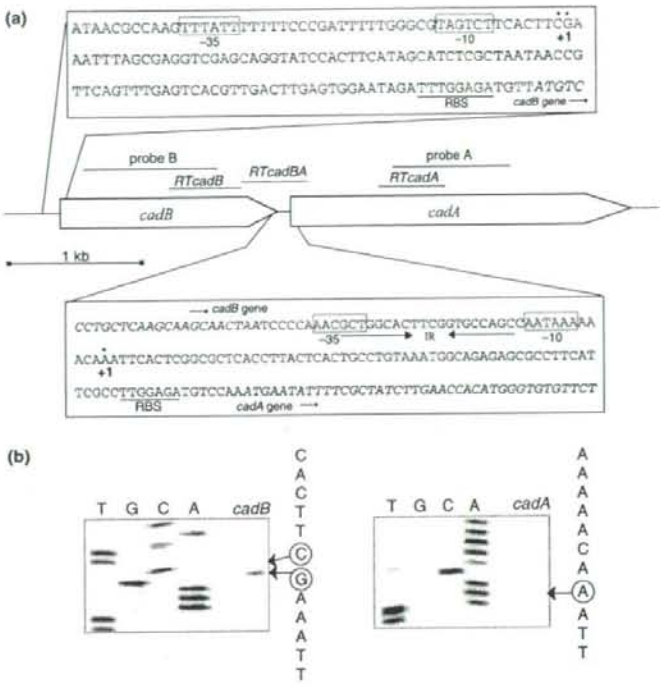

Figure 2 (a) Schematic representation of the *Vibrio parahaemolyticus* lysine decarboxylase gene cluster and intergenic region. Probes for the Northern blot hybridization of genes *cadB* and *cadA* and polymerase chain reaction (PCR) primers to measure mRNA species by quantitative reverse transcriptase (RT)-PCR are indicated by bars labelled with the probe name (probes B and A) and gene name (*RTcadB*, *RTcadBA*, and *RTcadA*), respectively. The *RTcadBA* fragment was targeted at the C-termini of *cadB* and *N*-termini of *cadA* to detect the bi-cistronic transcript. The periphery sequences of *cadB* and *cadA* are given in the inset. Protein coding regions are indicated by shading, the putative transcriptional terminator (inverted repeat, IR) is indicated by arrows, and the probable ribosome-binding site (RBS) is underlined. Transcriptional start sites (+1) of each gene is indicated by asterisks. Predicted promoter sites, −35 and −10, are indicated by boxes. The scale bar length of 1 kb of the sequence is indicated. (b) Primer extension analysis. The primer extension products with total RNA of *V. parahaemolyticus* were sized. Sequencing ladder obtained with the same primers were shown on the left.

expression of 0·198 ± 0·03, compared with 1·96 ± 0·89 for *cadB*, and 8·03 ± 0·08 for *cadA*. This suggests that the bi-cistronic transcript could not be visualized on Northern blot hybridization. The majority of the probe added to the total RNA might have been hybridized to the monocistronic transcripts because of their higher quantity (10- to 100-fold).

All data obtained from quantitative RT-PCR were normalized for cell numbers and extraction efficiency using the values for 16S rRNA endogenous control of 1 and 2·40 (with lysine) for pH 5·0, 0·738 and 0·643 (with lysine) for pH 5·5, and 0·487 and 0·683 (with lysine) for pH 7·5. No genomic DNA contamination was found in any of the RNA samples during 50 cycles of PCR with any of the primer pairs (data not shown).

Identification of the transcriptional start point of *cadA* and *cadB*

The transcriptional start point of *cad* genes of *V. parahaemolyticus* was determined, as shown in Fig. 2. The transcriptional start point of *cadB* mRNA was located 101 and 102 bases upstream from the start codon of *cadB*. The predicted promoter elements were TTTATT and TAGTCT located at −35 and −10, respectively. The *cadA* mRNA started from 75 bases upstream of the start codon, and the promoter elements were identified as follows: AACGCT at −35, AATAAA at −10. The promoter sequences of *cadA* and *cadB* have little resemblance to each other. Although these promoter elements have little similarity for the consensus sequences (TATAAT and TTGACA), except for the −10 box of *cadA*, they share significant homologies with the promoter elements of *V. chorelae cad* genes (Merrell and Camilli 2000).

Acid tolerance of *cadA* gene-inactivated strain

The acid tolerance of a mutant strain of the newly emergent *V. parahaemolyticus* clone, V02-64, serotype O3:K6 constructed with a disrupted *cadA* gene was also tested. The mutant strain has a plasmid integrated in its chromosome (single crossing over), with a corresponding decrease in lysine decarboxylating activity to 1/100 or less. The microscopic experiments, measurement of growth rate, and tests for biochemical properties using API ID32E (BioMerieux) revealed no changes to other characteristics by this manipulation. The 4·0-kb *Hin*cII fragment detected by southern blot hybridization using

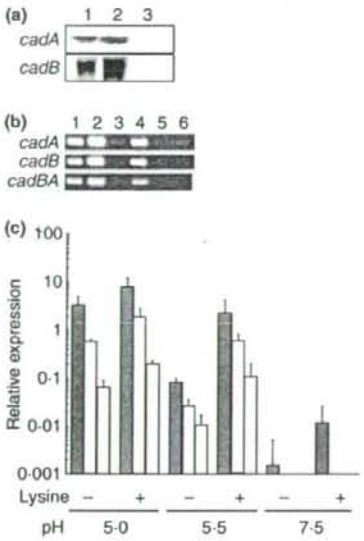

Figure 3 Transcriptional analysis of *cadBA* genes. (a) Northern blot hybridization analysis for *cadA* or *cadB* mRNA of *Vibrio parahaemolyticus* V02-64. Whole RNA (15 μg) was loaded, electrophoresed, blotted, and hybridized with probes specific for *cadA* or *cadB* under the following conditions: lane 1, pH 5·5; lane 2, pH 5·5 supplemented with 1% lysine; and lane 3, pH 7·5 with lysine. (b) Agarose gel images after 25 cycles of reverse transcriptase (RT)-polymerase chain reaction (PCR) under the following conditions: lane 1, pH 5·0; lane 2, pH 5·0 with lysine; lane 3, pH 5·5; lane 4, pH 5·5 with lysine; lane 5, pH 7·5; lane 6, pH 7·5 with lysine. (c) Relative expression analysis of *V. parahaemolyticus* lysine decarboxylase genes as detected by SYBR Green I real-time quantitative PCR under three pH conditions in the absence and presence of lysine. Total RNA extracted from the cells cultured in each condition was reverse transcribed by $d(N)_6$, and the quantity of cDNA consistent with that of the mRNA was quantified against a standard curve produced using genomic DNA. The relative amount of 1 is nearly equal to 10^4 copies of target DNA per 2 μl of the PCR template (=per reaction). Bars represent the averages of three to five experiments, and error bars indicate the SD (■, *cadA*; □, *cadB*; ▨, *cadBA*).

the *cadA* probe showed a band shift of 8·5 kb under the same conditions caused by plasmid integration in the mutant strain (data not shown). The acid resistance of this mutant strain at pH 4·0 in the phosphate buffer was weaker than in the parental strain; e.g. <0·01% of the mutant cells survived past 60 min of exposure, while 9·1% survival was observed for the wild-type strain (Fig. 4).

Discussion

The ATR is one of the strategies employed by the pathogens to infect and colonize mammalian hosts and has recently been reported in many enteropathogenic bacteria

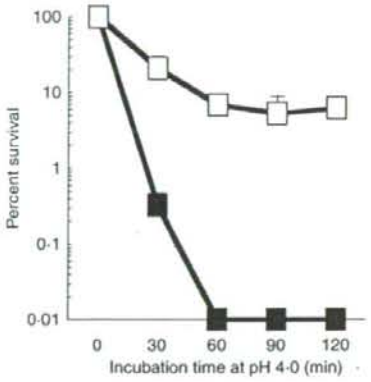

Figure 4 Acid resistance of the *Vibrio parahaemolyticus cadA* gene mutant and wild-type strains. All cell cultures were grown in Luria-Bertani (LB) media and collected at OD_{600} = 0·16–0·20 (log phase). Cells were all acid adapted in LB (pH 5·5) for 1 h to induce the acid-shock proteins. Acid-adapted cells were acid challenged in no citrate E medium (phosphate buffer, pH 4·0) with lysine at 37°C. Acid-challenged cells were then enumerated by plating onto trypticase soy agar medium at 30-min intervals. The survival of wild-type strain cells (open boxes) was reduced to one-tenths after 120 min, although survival of *cadA*-inactivated strain cells decreased immediately (closed boxes). Data represent the mean value of three measurements, and the error bars indicate the SD.

(Merrell and Camilli 2002). Among several proposed mechanisms of acid tolerance, amino acid decarboxylation has been confirmed in several bacteria. The molecular structure of lysine decarboxylase has been studied in some species, such as *E. coli* (Meng and Bennett 1992a,b), *S. typhimurium* (Foster and Hall 1991; Park *et al.* 1996), *V. cholerae* (Merrell and Camilli 1999, 2000), and *V. vulnificus* (Rhee *et al.* 2002). Among these species, lysine decarboxylase was confirmed to play a role in ATR in all but *E. coli*. Instead, *E. coli* utilizes glutamate decarboxylase as an alternative amino acid decarboxylase for ATR (Lin *et al.* 1995). Further, Samartzidou *et al.* (2003) have demonstrated that cadaverine, decarboxylated from lysine, plays a role in acid survival through porin inhibition in *E. coli*.

To achieve ATR via amino acid decarboxylation, two or more enzymes appear to be necessary (Bearson *et al.* 1997; Merrell and Camilli 2002); decarboxylation enzymes and their antiporters facilitate the coupled transport of amino acids and their decarboxylation products across the membrane. Each decarboxylation reaction consumes one intracellular proton to generate products including γ-aminobutyric acid (from glutamic acid) and cadaverine (from lysine), which are excreted to the extracellular space by antiporter protein and thereby decrease the

intracellular proton concentration and protect the cells from external acid stress. In our study, the molecular structure of the lysine decarboxylase gene cluster of *V. parahaemolyticus* was determined. Two ORF having sequences of 2136 and 1344 bp were identified as lysine decarboxylase (*cadA*) and lysine/cadaverine antiporter (*cadB*), respectively (Fig. 2a).

ATR of *V. parahaemolyticus* under low pH conditions is largely dependent on the presence of external lysine. Acid-adapted *V. parahaemolyticus* is resistant to low pH (4·0) only in the presence of external lysine (Fig. 1). Further, this adaptation effect is inhibited by chloramphenicol, an inhibitor of protein synthesis. Similar results have been obtained for all tested strains of *V. parahaemolyticus*, and these data suggest that *V. parahaemolyticus* gains resistance to conditions of low pH by using lysine and synthesizing proteins and that lysine-dependent pathways contribute significantly to the ATR of this pathogen. Thus, our findings corroborated previous reports that *V. parahaemolyticus* has the ability to mount a robust ATR, largely dependent on the presence of lysine.

In this study, transcriptional analyses by Northern blot hybridization and quantitative RT-PCR revealed that the *cad* genes of *V. parahaemolyticus* form an acid-inducible operon, while individual transcripts of *cadB* and *cadA* were also observed (Fig. 3a,b). The strength of induction of *cad* genes, which are related to acid adaptation, was shown to be inversely proportional to pH, suggesting that lysine decarboxylase genes are also responsible for the ATR of *V. parahaemolyticus*. The acid-inducible properties of the *cad* genes are the same in both *E. coli* and *V. cholerae*, the former has only a bi-cistronic transcript (Meng and Bennett 1992b), while the latter produces three transcripts comprising *cadBA*, *cadB*, and *cadA* (Merrell and Camilli 1999, 2000).

A small amount of *cadA* transcript is still produced under neutral pH conditions (Fig. 3c). This constitutive expression might be the result of substitution of another lysine decarboxylase (biosynthetic) found in *E. coli* (Kikuchi *et al.* 1997) as no other lysine decarboxylase was found in the entire genome of *V. parahaemolyticus* by southern hybridization (this study, data not shown) and whole genome sequencing (Makino *et al.* 2003). Cadaverine has been reported to play a role in the control of outer membrane permeability (Samartzidou *et al.* 2003) and cell division (Pruss *et al.* 1997) in *E. coli*. Therefore, decarboxylase protein CadA, the most important protein in the decarboxylation pathway, is expressed solely under neutral pH for the adjustment of the intracellular lysine or cadaverine concentration, although the expression level is low.

While the *cadB* and *cadA* genes of *V. parahaemolyticus* form an operon construct, the expression ratio between *cadB*, *cadA*, and *cadBA* was *c.* 10 : 100 : 1. The probable transcriptional terminator, the inverted repeat sequence of the *cadB* gene is indicated in Fig. 2a. Because this terminator-like sequence has sufficient length similar to a stem and a loop and includes several bases of the poly-A region, it is reasonable to assume that it acts as a transcription terminator. This likely explains the low production of *cadBA* mRNA, which is transcribed from the promoter upstream of *cadB* to the terminator of *cadA*. The *cadA* mRNA, the most abundant of the transcripts, is transcribed using its own upstream promoter. The predicted promoter regions of *cadB* and *cadA* have little resemblance. While both are acid-inducible promoters, differing transcriptional pattern were observed between *cadB* and *cadA* genes. The promoter sequence of *cadA* was more similar to the consensus sequence than that of *cadB* (Fig. 2a). Therefore, we consider that the *cadA* sole transcript is generated by its own promoter because the activity of promoter of *cadA* might be strong. When cells encounter low pH stress, *cadA* expression is increased and the *cadB* gene, which is indispensable in effecting acid tolerance, is also expressed. Some portion of the *cadB* transcripts do not terminate at the terminator located on the *cadB–cadA* intergenic region, and, thus, *cadBA* bi-cistronic transcripts are produced. In this study, the cadC-like ORF was observed in *V. parahaemolyticus* (data not shown). As *cadC* is reported to be a positive transcriptional regulator of the *cadBA* operon (Merrell and Camilli 2000; Rhee *et al.* 2005), the transcription of *cadBA* genes of *V. parahaemolyticus* might be regulated in the same way. The transcriptional regulation of the *V. parahaemolyticus cadBA* operon will be studied further.

To summarize, in the transcription of the *V. parahaemolyticus cad* operon, the *cadA* gene is constitutively expressed while *cadB* is not. Under low pH, the *cadA* gene is highly expressed, the *cadB* gene is also transcribed, and *cadB–cadA* bi-cistronic transcript is occasionally produced. This transcriptional regulation occurs because different amounts of CadA and CadB are required.

The mutant strain, with a disrupted *cadA* gene, was constructed to verify the role of *cadA* in ATR. The mutant strain was shown to have inactivated the *cadA* gene by an indicator broth, along with HPLC method, PCR, southern blot hybridization, and DNA sequencing (data not shown). All results showed the plasmid integration into the interior of the *cadA* gene, although a little cadaverine was detected from overnight cultures of the mutant strain. This remaining activity is speculated to be the result of imperfect mutation caused by the plasmid remaining in the chromosome. This mutant strain showed higher acid sensitivity than the wild-type strain, although other characteristics (growth rate, requirements for nutrition, biochemical characteristics, and colony

morphology) did not change. This mutant showed 1/1000 the acid resistance of wild-type strains under our experimental conditions. This indicates that lysine decarboxylation plays a role in the acid resistance of *V. parahaemolyticus*. This mechanism is generally considered to be related to the decreasing intracellular proton concentration through the decarboxylation reaction, and improvement of the microenvironment by excretion of the basic molecule, amine. This model has been proposed by many authors, although to the best of our knowledge, it has not been experimentally proven so far. Thus, further study is required to further develop this model. Alternatively, OmpU, an outer membrane protein, mediates organic acid resistance in *V. cholerae* (Merrell *et al.* 2001). Merrell *et al.* (2001) reported that this was accomplished by inhibition of the permeation of organic acid molecules. OMP-mediated acid resistance was also reported in *E. coli* (Samartzidou *et al.* 2003).

In conclusion, we have identified lysine decarboxylating pathway as the factor that allows survival under acidic conditions. This was confirmed by gene mutation analysis and mRNA quantification through SYBR Green I real-time RT-PCR that precisely determined the transcriptional aspects of *V. parahaemolyticus cad* genes. Acid resistance is universal in *V. parahaemolyticus* and the level does not diverge among strains. Recently, *V. parahaemolyticus* serotype O3:K6, which originated from a single clone, is spreading worldwide. Although some enhanced factor(s) might be involved in the pandemic spread of this pathogen, acid resistance is not.

Acknowledgements

This work was partly supported by the National Food Research Institute of Japan (project: Development of evaluation and management methods for supply of safe, reliable and functional food and farm produce) and the Japanese Ministry of Health, Labour and Welfare (H19–011).

The authors thank Yohko Sekine for technical assistance.

References

Audia, J.P., Webb, C.C. and Foster, J.W. (2001) Breaking through the acid barrier: an orchestrated response to proton stress by enteric bacteria. *Int J Med Microbiol* **291**, 97–106.

Bearson, S., Bearson, B. and Foster, J.W. (1997) Acid stress responses in enterobacteria. *FEMS Microbiol Lett* **147**, 173–180.

Bennish, M.L. (1994) Cholera: pathophysiology, clinical features, and treatment. In *Vibrio cholerae and Cholera: Molecular to Global Perspectives* ed. Wachsmuth, K.I., Blake, P.A. and Olsik, O. pp. 229–255. Washington, DC: American Society for Microbiology.

Centers for Disease Control and Prevention. (1998) Outbreak of *Vibrio parahaemolyticus* infections associated with eating raw oysters - Pacific Northwest, 1997. *Morbid Mortal Weekly Rep* **47**, 457–462.

Centers for Disease Control and Prevention. (1999) Outbreak of *Vibrio parahaemolyticus* infection associated with eating raw oysters and clams harvested from Long Island Sound – Connecticut, New Jersey, and New York, 1998. *Morbid Mortal Weekly Rep* **48**, 48–51.

Daniels, N.A., MacKinnon, L., Bishop, R., Altekruse, S., Ray, B., Hammond, R.M., Thompson, S., Wilson, S., *et al.* (2000) *Vibrio parahaemolyticus* infections in the United States, 1973–1998. *J Infect Dis* **181**, 1661–1666.

DePaola, A., Hopkins, L.H., Peeler, J.T., Wentz, B. and McPhearson, R.M. (1990) Incidence of *Vibrio parahaemolyticus* in U.S. coastal waters and oysters. *Appl Environ Microbiol* **56**, 2299–2302.

Faruque, S.M., Albert, M.J. and Mekalanos, J.J. (1998) Epidemiology, genetics, and ecology of toxigenic *Vibrio cholerae*. *Microbiol Mol Biol Rev* **62**, 1301–1314.

Foster, J.W. (1999) When protons attack: microbial strategies of acid adaptation. *Curr Opin Microbiol* **2**, 170–174.

Foster, J.W. and Hall, H.K. (1990) Adaptive acidification tolerance response of *Salmonella typhimurium*. *J Bacteriol* **172**, 771–778.

Foster, J.W. and Hall, H.K. (1991) Inducible pH homeostasis and the acid tolerance response of *Salmonella typhimurium*. *J Bacteriol* **173**, 5129–5135.

Honda, T. and Iida, T. (1993) The pathogenicity of *Vibrio parahaemolyticus* and the role of the thermostable direct hemolysin and related hemolysins. *Rev Med Microbiol* **4**, 106–113.

Joseph, S.W., Colwell, R.R. and Kaper, J.B. (1982) *Vibrio parahaemolyticus* and related halophilic vibrios. *Crit Rev Microbiol* **10**, 77–124.

Kaysner, C.A., Abeyta, C. Jr, Stott, R.F., Lilja, J.L. and Wekell, M.M. (1990) Incidence of urea-hydrolyzing *Vibrio parahaemolyticus* in Willapa Bay, Washington. *Appl Environ Microbiol* **56**, 904–907.

Kikuchi, Y., Kojima, H., Tanaka, T., Takatsuka, Y. and Kamio, Y. (1997) Characterization of a second lysine decarboxylase isolated from *Escherichia coli*. *J Bacteriol* **179**, 4486–4492.

Lin, J., Lee, I.S., Frey, J., Slonczewski, J.L. and Foster, J.W. (1995) Comparative analysis of extreme acid survival in *Salmonella typhimurium*, *Shigella flexneri*, and *Escherichia coli*. *J Bacteriol* **177**, 4097–4104.

Makino, K., Oshima, K., Kurokawa, K., Yokoyama, K., Uda, T., Tagomori, K., Iijima, Y., Najima, M., *et al.* (2003) Genome sequence of *Vibrio parahaemolyticus*: a pathogenic mechanism distinct from that of *V. cholerae*. *Lancet* **361**, 743–749.

Maloy, S.R. and Roth, J.R. (1983) Regulation of proline utilization in *Salmonella typhimurium*: characterization of

put::Mu *d* (Ap, *lac*) operon fusions. *J Bacteriol* **154**, 561–568.

Matsumoto, C., Okuda, J., Ishibashi, M., Iwanaga, M., Garg, P., Rammamurthy, T., Wong, H.C., Depaola, A., *et al.* (2000) Pandemic spread of an O3:K6 clone of *Vibrio parahaemolyticus* and emergence of related strains evidenced by arbitrarily primed PCR and *toxRS* sequence analysis. *J Clin Microbiol* **38**, 578–585.

Meng, S.Y. and Bennett, G.N. (1992a) Nucleotide sequence of the *Escherichia coli cad* operon: a system for neutralization of low extracellular pH. *J Bacteriol* **174**, 2659–2669.

Meng, S.Y. and Bennett, G.N. (1992b) Regulation of the *Escherichia coli cad* operon: location of a site required for acid induction. *J Bacteriol* **174**, 2670–2678.

Merrell, D.S. and Camilli, A. (1999) The *cadA* gene of *Vibrio cholerae* is induced during infection and plays a role in acid tolerance. *Mol Microbiol* **34**, 836–849.

Merrell, D.S. and Camilli, A. (2000) Regulation of *Vibrio cholerae* genes required for acid tolerance by a member of the "ToxR-like" family of transcriptional regulators. *J Bacteriol* **182**, 5342–5350.

Merrell, D.S. and Camilli, A. (2002) Acid tolerance of gastrointestinal pathogens. *Curr Opin Microbiol* **5**, 51–55.

Merrell, D.S., Bailey, C., Kaper, J.B. and Camilli, A. (2001) The *toxR*-mediated organic acid tolerance response of *Vibrio cholerae* requires OmpU. *J Bacteriol* **183**, 2746–2754.

Naim, R., Yanagihara, I., Iida, T. and Honda, T. (2001) *Vibrio parahaemolyticus* thermostable direct hemolysin can induce an apoptotic cell death in Rat-1 cells from inside and outside of the cells. *FEMS Microbiol Lett* **195**, 237–244.

Nasu, H., Iida, T., Sugahara, T., Yamaichi, Y., Park, K.S., Yokoyama, K., Makino, K., Shinagawa, H., *et al.* (2000) A filamentous phage associated with recent pandemic *Vibrio parahaemolyticus* O3:K6 strains. *J Clin Microbiol* **38**, 2156–2161.

Nishikawa, Y., Ogasawara, J. and Kimura, T. (1993) Heat and acid sensitivity of motile *Aeromonas*: a comparison with other food-poisoning bacteria. *Int J Food Microbiol* **18**, 271–278.

Park, Y.K., Bearson, B., Bang, S.H., Bang, I.S. and Foster, J.W. (1996) Internal pH crisis, lysine decarboxylase and the acid tolerance response of *Salmonella typhimurium*. *Mol Microbiol* **20**, 605–611.

Pruss, B.M., Markovic, D. and Matsumura, P. (1997) The *Escherichia coli* flagellar transcriptional activator *flhD* regulates cell division through induction of the acid response gene *cadA*. *J Bacteriol* **179**, 3818–3821.

Raimondi, F., Kao, J.P., Fiorentini, C., Fabbri, A., Donelli, G., Gasparini, N., Rubino, A. and Fasano, A. (2000) Enterotoxicity and cytotoxicity of *Vibrio parahaemolyticus* thermostable direct hemolysin in *in vitro* systems. *Infect Immun* **68**, 3180–3185.

Rhee, J.E., Kim, K.H. and Choi, S.H. (2005) CadC activates pH-dependent expression of the *Vibrio vulnificus cadBA* operon at a distance through direct binding to an upstream region. *J Bacteriol* **187**, 7870–7875.

Rhee, J.E., Rhee, J.H., Ryu, P.Y. and Choi, S.H. (2002) Identification of the *cadBA* operon from *Vibrio vulnificus* and its influence on survival to acid stress. *FEMS Microbiol Lett* **208**, 245–251.

Samartzidou, H., Mehrazin, M., Xu, Z., Benedik, M.J. and Delcour, A.H. (2003) Cadaverine inhibition of porin plays a role in cell survival at acidic pH. *J Bacteriol* **185**, 13–19.

Sambrook, J.E., Fritsch, F. and Maniatis, T.S. (1989) *Molecular Cloning: A Laboratory Manual*, 2nd edn. Cold Spring Harbor, New York: Cold Spring Harbor Laboratory.

Sanyal, S.C. and Sen, P.C. (1974) Human volunteer study on the pathogenicity of *Vibrio parahaemolyticus*. In *International Symposium of Vibrio parahaemolyticus* ed. Fujino, T., Sakaguchi, G., Sakazaki, R. and Takeda, Y. pp. 227–230. Tokyo: Saikon Publishing Co., Ltd.

Shimada, T. and Arakawa, E. (2000) Current status of *Vibrio parahaemolyticus* food poisoning. *J Antibact Antifung Agents* **28**, 157–167.

Wagatsuma, S. (1974) Ecological studies on Kanagawa phenomenon positive strains of *Vibrio parahaemolyticus*. In *International Symposium of Vibrio parahaemolyticus* ed. Fujino, T., Sakaguchi, G., Sakazaki, R. and Takeda, Y. pp. 91–96. Tokyo: Saikon Publishing Co., Ltd.

Waterman, S.R. and Small, P.L.C. (1998) Acid-sensitive enteric pathogens are protected from killing under extremely acidic conditions of pH 2·5 when they are inoculated onto certain solid food sources. *Appl Environ Microbiol* **64**, 3882–3886.

Wilmes-Riesenberg, M.R., Bearson, B., Foster, J.W. and Curtiss, R. III (1996) Role of acid tolerance response in virulence of *Salmonella typhimurium*. *Infect Immun* **64**, 1085–1092.

Wong, H., Peng, P., Han, J., Chang, C. and Lan, S. (1998) Effect of mild acid treatment on the survival, enteropathogenicity, and protein production in *Vibrio parahaemolyticus*. *Infect Immun* **66**, 3066–3071.

Xu, M., Yamamoto, K. and Honda, T. (1994) Construction and characterization of an isogenic mutant of *Vibrio parahaemolyticus* having a deletion in the thermostable direct hemolysin-related hemolysin gene (*trh*). *J Bacteriol* **176**, 4757–4760.

Yamanaka, H. and Matsumoto, M. (1989) Simultaneous determination of polyamines in red meat fishes by high performance liquid chromatography and evaluation of freshness. *J Food Hyg Soc Jpn* **30**, 396–400.

Journal of Food Protection, Vol. 71, No. 3, 2008, Pages 468–472

Growth and Toxin Production of Proteolytic *Clostridium botulinum* in Aseptically Steamed Rice Products at pH 4.6 to 6.8, Packed under Modified Atmosphere, Using a Deoxidant Pack

BON KIMURA,[1]* RYUSUKE KIMURA,[1] TETSUYA FUKAYA,[2] KINYA SAKUMA,[3] SATOKO MIYA,[1] AND TATEO FUJII[1]

[1]*Department of Food Science and Technology, Faculty of Marine Science, Tokyo University of Marine Science and Technology, 4-5-7 Konan, Minato, Tokyo 108-8477, Japan;* [2]*Food Product R and D Group, Research Institute, Kagome Company, Limited, Naka-ku Nagoya, Aichi 460-0003, Japan; and* [3]*Research and Development Section, Nitto Aliment Company, Limited, Shibata, Nigata 957-0356, Japan*

MS 07-333: Received 26 June 2007/Accepted 5 November 2007

ABSTRACT

Demand for aseptically steamed rice products has been increasing rapidly in Japan over the past 10 years. In our previous study, we showed that proteolytic *Clostridium botulinum* produce toxins in steamed rice products packaged under a modified atmosphere of ≤0.3% oxygen. In the present study, we examined the effect of pH to control botulism risk in steamed rice products packaged under modified atmosphere (5% CO_2 and 95% N_2 as the balance) with the inclusion of a deoxidant pack to produce an oxygen concentration of ≤0.3%. A mixture of 10 strains of proteolytic *C. botulinum* (5 type A strains and 5 type B strains) was inoculated into steamed rice products at pH values between 4.6 and 6.8 prior to packaging. All samples were stored at 30°C for 24 weeks. Samples at higher pH showed earlier starts of neurotoxin production. Neurotoxin was detected after 2 weeks of incubation in samples at pH 5.4 or above, whereas it took 4 weeks for the toxin to be detected in samples at pH 5.2 to 5.3 and 12 weeks in samples at pH 5.0 to 5.1. In samples at pH 4.9 or below, no toxin was detected during the experimental period. Apparent sample spoilage did not occur before *C. botulinum* produced neurotoxin in most of the samples. Based on these results, we conclude that aseptically steamed rice products must be packaged at pH 4.9 or below under modified atmosphere containing ≤0.3% oxygen, with the inclusion of a deoxidant pack.

Aseptic packaging, which is commonly used for milk, soup, pasta, and other foods, has also been used for steamed rice products in Japan. Packaged rice products can be stored for 6 months, or even longer, at room temperature and only require microwave oven heating preparation. These products are often packed under modified atmosphere: some contain 5 to 10% oxygen, and some are packed under modified atmosphere with the inclusion of a deoxidant pack so that oxygen concentration nearly reaches 0%. Modified atmosphere packaging (MAP) has become a popular means of extending shelf life of precooked foods, such as fresh pork *(12)*, fish fillets *(10, 13)*, vegetables *(6, 11, 16)*, and other food items *(3, 17)*, by preventing growth of aerobic bacteria, molds, and yeasts. However, MAP may permit growth of and toxin production by anaerobic spore-forming bacteria such as *Clostridium botulinum*. Although aseptically steamed rice products are packaged after cooking and steam sterilization, using an ultrahigh-temperature flash-heating process (generally ≥8 s at 135°C; $F_0 > 3.1$) to eliminate primary contamination, these products still carry a slight risk of secondary contamination of *C. botulinum* spores. In fact, production of neurotoxin by proteolytic *C. botulinum* was demonstrated in commercially manufactured steamed rice with MAP (pH 6.5) *(8)*. In our previous study *(8)*, therefore, we examined the effect of oxygen concentration on preventing toxin production by this pathogen in these products, and we determined 10% oxygen to be most effective. However, we still considered lower oxygen concentrations to be desirable in order to inhibit the growth of aerobic microorganisms. In fact, atmospheric conditions of nearly 0% oxygen with the inclusion of a deoxidant pack has already been adapted for the manufacture of some of these products in Japan in order to prevent the growth of aerobes, including molds.

When *C. botulinum* spores alone were inoculated into a medium made from cooked meat medium, toxin production was strictly limited below pH 4.6 *(21)*. However, since aseptically steamed rice products with pH adjusted below 4.6 taste acidic, most products currently distributed in Japan have a higher pH, mostly around 6.5.

In this study, we examined the pH threshold for controlling the risk of *C. botulinum* packaging that achieves ≤0.3% oxygen concentration through the used of modified atmosphere and the inclusion of deoxidant pack. To determine the safety level of pH that prevents *C. botulinum*–toxin production, proteolytic *C. botulinum* (types A and B) were inoculated into steamed rice adjusted to pH values between 4.6 and 6.8.

MATERIALS AND METHODS

Bacterial strains. Five type A strains (56A, 62A, 97A, Hall A, and Renkon-1 A) and five type B strains (9B, 213B, 407-1 B,

* Author for correspondence. Tel: +81-3-5463-0603; Fax: +81-3-5463-0603; E-mail: kimubo@kaiyodai.ac.jp.

Fukuyama B, and Okra B) of proteolytic group I were used in this study. The 56A, Hall A, Renkon-1 A, 213 B, 407-1 B, and Fukuyama B strains were kindly provided from the culture collection of H. Nakano (Laboratory of Food Microbiology and Hygiene, Hiroshima University, Hiroshima, Japan). The other *C. botulinum* strains (62A, 97A, 9B, and Okra B (proteolytic, group I) were kindly provided by the National Institute of Infectious Diseases (Tokyo, Japan).

Rice samples. Steamed, sterilized rice was prepared in a pilot plant. Briefly, after the rice bran had been sufficiently removed, the rice was washed and soaked in water for 30 min. After removing the water, the rice was steam sterilized using an ultrahigh-temperature flash-heating process (generally ≥8 s at 135°C; $F_0 >$ 3.1), followed by cooling. Packaging and the entire processing beyond the sterilization were carried out in a clean room (class 1,000). The sterilized rice was soaked in sterilized cooking water adjusted using gluconic acid to yield steamed rice with a pH of 4.6 to 6.8. The pH of water before cooking was equal to the pH of rice after cooking. And the rice was cooked at a rice:water ratio of 1:1 to produce a final cooked product with a water content of 60% (water activity of 0.98 to 0.99), which is representative of commercial products currently distributed in Japan. The soaked rice was then steam cooked at approximately 100°C, without controlling pressure for 30 min. The color of the acidically adjusted rice did not change after cooking, and it was identical to rice cooked normally. The steam-cooked rice was then aseptically packed in commercial packaging, with sample sizes of approximately 110 g, using a plastic plate and aseptically sealing with plastic film. These rice samples were stored at 30°C for 1 week and were visually inspected prior to inoculation with *C. botulinum*.

Preparation of *C. botulinum* spores. Preparation of *C. botulinum* spores and the subsequent enumeration were conducted under anaerobic conditions. *C. botulinum* strains were precultured in cooked meat medium (Eiken Chemical Co., Tokyo, Japan) at 37°C overnight. Spores of each strain were produced at 37°C over 7 days in Trypticase Peptone yeast broth (pH 7.0) with 5% (wt/vol) Trypticase Peptone (Difco, Becton Dickinson, Sparks, Md.), 0.5% (wt/vol) Bacto Peptone (Difco, Becton Dickinson), and 0.1% (wt/vol) Bacto yeast extract (Difco, Becton Dickinson). Before harvest, spores were checked with a phase contrast microscope (Olympus Co., Tokyo, Japan) for the dominance of refractile spores (>90%). Spore crops of each strain were centrifuged at 21,480 × *g* for 10 min at 4°C (SRX-201, Tomy Seiko Co., Tokyo Japan), and pellets were washed with sterile distilled water. Each crop was resuspended in sterile distilled water and frozen at −20°C until use. Spores of each strain were counted by the three-tube most-probable-number method after heat-shock treatment (80°C for 10 min, followed by rapid cooling).

Inoculation with *C. botulinum*. Equal numbers of *C. botulinum* spores from each of 10 different strains were mixed and adjusted to a concentration of approximately 4 log spores per ml. The spore mixtures were heat shocked (80°C for 10 min, followed by rapid cooling) and then 100 μl of the spore mixture was inoculated into each rice sample at each of 10 points (total of 1 ml of inoculum per rice sample) to avoid contingency differences among the samples. Cell counts of the samples and time-zero inoculum were determined by the serial dilution and pouch method *(2, 5)*, using clostridia count agar (Nissui Pharmaceutical Co., Tokyo, Japan). Inoculated samples were packaged in high-gas-barrier film bags (Basela, Kureha Chemical Industry Co., Tokyo, Japan), using a Tospack V 400 gas changer (Tosei, Ohito, Shizuoka, Japan) along with a deoxidant pack (Mitsubishi Gas Chemical Co., Inc., Tokyo, Japan) under atmospheric conditions of 0% oxygen, 5% carbon dioxide, and 95% nitrogen. All samples were incubated at 30°C. The samples were tested at weeks 0, 2, 4, 12, and 24. All the experiments were conducted in triplicate.

pH and atmospheric composition measurements. Headspace gas was analyzed for the concentration of carbon dioxide and oxygen, using a G5000A gas chromatograph (Hitachi, Tokyo, Japan). Subsamples (10 g) were placed in plastic bags (80 ml; Organo Co., Tokyo, Japan) with 10 ml of sterilized distilled water and mixed by hand for approximately 1 min to achieve a sufficiently homogeneous mixture without damaging the rice grains. Prior to the experiments, we confirmed that hand mixing was sufficient to mix the samples for microbiological counts while avoiding shredding rice grains as occurs when samples are mixed with a stomacher. pH was measured with a glass electrode pH meter (Horiba, Kyoto, Japan). The remainder of each sample (approximately 100 g) was placed in a stomacher bags (400 ml; Organo) with 100 ml of sterilized phosphate buffer (0.4% [wt/vol] Na_2HPO_4 and 0.2% [wt/vol] gelatin, pH 6.2) and mixed by hand (1 to 2 min). A portion of the mixture was used for microbiological analysis, and approximately 13 ml was transferred to sterilized centrifuge tubes (15 ml; Labcon, Petaluma, Calif) and stored at −20°C until neurotoxin assay.

Sensory evaluation. After incubation, the packages were opened, and the appearance and odor of the samples were assessed for spoilage by a panel of five judges with no special training. A sample was regarded as spoiled when all five people judged the sample as inedible, but an edible judgment by just one person was sufficient to consider the sample unspoiled.

Microbiological analysis. Anaerobic cell counts were carried out by serial dilution and pouch methods *(2, 5)* with Clostridia count agar. Portions of the same samples were used for contamination checks on PCA (Eiken) by the pour-plate method. Uninoculated samples were also checked for aerobic and anaerobic counts to confirm the absence of all bacteria.

Neurotoxin assay. Frozen rice samples were thawed, mixed, and centrifuged at 2,190 × *g* for 10 min. Two mice (approximately 20 g) were each intraperitoneally injected with 0.5 ml of supernatant. Samples were considered toxic if typical respiratory symptoms of botulism occurred and both mice died during the 48-h observation period *(19)*. For samples producing toxic reactions, neurotoxin was tested for serum type by inoculating sample into mice protected with A and/or B antiserum (two mice for each treatment; six mice total) (Chiba Serum Institute, Chiba, Japan). Following the manufacturer's instructions, antiserum protection was established with a 0.5-ml intraperitoneal injection of 2 U/ml adjusted type A and/or B antiserum and the same volume of sample incubated for 1 h at room temperature. If mice protected with B antiserum died while those protected with A antiserum lived during the 48-h observation period, then the toxin was considered to be type A. Conversely, if mice protected with A antiserum died while those protected with B antiserum lived, then the toxin was considered to be type B. If mice protected with both A and B antiserum lived while the other mice died, then both toxin types A and B were considered present.

RESULTS

Measurements of pH and atmospheric composition. Atmospheric composition and pH values are shown in Table 1. The oxygen concentration at the time of packaging

TABLE 1. *Analysis of rice samples inoculated with* Clostridium botulinum *(type A, B) spores*[a]

Initial pH	Incubation time (wk)	No. of samples spoiled/no. of samples tested	Sample with toxin	Sample parameters				
				pH	O_2 (%)	CO_2 (%)	Anaerobic count (log CFU/g)	Anaerobic count (log CFU/g)[b]
4.6–4.7	0	0/1	ND[c]	4.7	0.8	1.8	2.1	ND
	2	0/3	ND	4.7 ± 0.0	0.2 ± 0.0	0.0 ± 0.0	2.1 ± 0.1	ND
	4	0/3	ND	4.7 ± 0.1	0.2 ± 0.1	0.0 ± 0.0	2.0 ± 0.0	ND
	12	0/3	ND	4.8 ± 0.1	0.2 ± 0.1	0.0 ± 0.0	1.8 ± 0.1	ND
	24	0/3	ND	4.8 ± 0.1	0.1 ± 0.1	0.0 ± 0.0	1.9 ± 0.0	ND
4.8–4.9	0	0/1	ND	4.9	0.8	1.8	2.1	ND
	2	0/3	ND	4.8 ± 0.1	0.2 ± 0.0	0.0 ± 0.0	2.3 ± 0.1	ND
	4	0/3	ND	5.0 ± 0.0	0.2 ± 0.1	0.0 ± 0.0	2.0 ± 0.0	ND
	12	0/3	ND	5.0 ± 0.1	0.3 ± 0.2	0.0 ± 0.0	1.9 ± 0.1	ND
	24	0/3	ND	5.0 ± 0.0	0.1 ± 0.0	0.0 ± 0.0	2.5 ± 0.2	ND
5.0–5.1	0	0/1	ND	5.2	0.8	1.5	2.1	ND
	2	0/3	ND	5.1 ± 0.0	0.2 ± 0.0	0.0 ± 0.0	2.3 ± 0.3	ND
	4	0/3	ND	5.2 ± 0.0	0.2 ± 0.1	0.0 ± 0.0	2.0 ± 0.1	ND
	12	0/2	ND	5.5 ± 0.0	0.2 ± 0.1	0.0 ± 0.0	2.0 ± 0.1	ND
		0/1	A	5.6	0.3	0	3.8	ND
	24	0/3	A (3/3)[d]	5.4 ± 0.0	0.1 ± 0.0	0.0 ± 0.0	4.2 ± 0.2	ND
5.2–5.3	0	0/1	ND	5.4	0.8	1.6	2.1	ND
	2	0/3	ND	5.3 ± 0.0	0.2 ± 0.0	0.0 ± 0.0	4.4 ± 0.1	ND
	4	0/3	A (1/3)[e]	5.4 ± 0.1	0.3 ± 0.1	0.0 ± 0.0	4.5 ± 1.1	ND
	12	0/3	ND	5.5 ± 0.1	0.2 ± 0.1	0.0 ± 0.0	2.7 ± 0.6	ND
	24	0/3	A (3/3)	5.5 ± 0.1	0.1 ± 0.1	0.0 ± 0.0	4.4 ± 0.0	ND
5.4–5.5	0	0/1	ND	5.5	0.8	1.6	2.1	ND
	2	0/3	A (3/3)	5.5 ± 0.0	0.2 ± 0.0	0.0 ± 0.0	4.9 ± 0.0	ND
	4	0/3	A+B (3/3)	5.6 ± 0.1	0.2 ± 0.0	0.0 ± 0.0	4.7 ± 0.1	ND
5.6–5.7	0	0/1	ND	5.6	0.8	1.6	2.1	ND
	2	0/3	A+B (3/3)	5.7 ± 0.1	0.2 ± 0.0	0.0 ± 0.0	5.4 ± 0.1	ND
	4	ND	ND	ND	ND	ND	ND	ND
5.8–5.9	0	0/1	ND	5.9	0.8	1.7	2.1	ND
	2	0/3	A+B (3/3)	5.9 ± 0.1	0.2 ± 0.0	0.0 ± 0.0	5.6 ± 0.0	ND
	4	ND	ND	ND	ND	ND	ND	ND
6.0–6.1	0	0/1	ND	6.1	0.8	1.6	2.1	ND
	2	0/3	A+B (3/3)	6.0 ± 0.1	0.2 ± 0.0	0.0 ± 0.0	5.6 ± 0.2	ND
	4	ND	ND	ND	ND	ND	ND	ND
6.2–6.3	0	0/1	ND	6.2	0.8	1.7	2.1	ND
	2	0/3	A+B (3/3)	6.2 ± 0.1	0.2 ± 0.0	0.0 ± 0.0	6.2 ± 0.0	ND
	4	ND	ND	ND	ND	ND	ND	ND
6.8–6.9	0	0/1	ND	6.8	0.8	1.7	2.1	ND
	2	3/3	A+B (3/3)	6.8 ± 0.1	0.2 ± 0.0	0.0 ± 0.0	6.8 ± 0.1	ND
	4	ND	ND	ND	ND	ND	ND	ND

[a] Rice sample had 60% water content.
[b] The limit of detection of viable count is 2 CFU/g.
[c] ND, not detected.
[d] Toxin was detected (0.1% oxygen, pH 5.4) in all three samples.
[e] Toxin was detected (0.3% oxygen, pH 5.4) in one of three samples.

was 0.8%, and it dropped to ≤0.3% after 2 weeks in all samples. The initial carbon dioxide concentration was 1.8%, but no CO_2 was detected after 2 weeks of incubation in all sample types. There was no significant change in the sample pH value over 24 weeks.

Growth of *C. botulinum* in steamed rice. Growth of *C. botulinum* in steamed rice at 30°C is shown in Table 1. Anaerobic counts were assumed to equal the *C. botulinum* counts because rice samples were supposed to be sterile in the absence of *C. botulinum* inoculation. Initial *C. botulinum* counts were an average 2.1 log CFU/g for all sample types. Counts after 2 weeks of incubation increased significantly in samples initially adjusted to pH 5.2 or above, ranging from 4.4 log CFU/g in samples at pH 5.2 to 6.8 log CFU/g in samples at pH 6.8. The only exception was samples at pH 5.2 to 5.3 collected at week 12, in which the anaerobic counts were lower than the counts of those collected at week 4. Sample spoilage occurred only in samples at pH 6.8. Increases in anaerobic counts were also detected in samples of lower pH later in the experimental period. One of the samples at pH 5.0 showed an increased anaerobic count of 3.8 log CFU/g after 12 weeks of incubation

and an anaerobic count of 4.2 log CFU/g was detected in all three samples.

No bacterial growth was detected by aerobic cell counts in any of the samples, as expected.

Neurotoxin assay. Neurotoxin detection data are shown in Table 1. The higher the sample pH value, the earlier the start of neurotoxin production was observed. Neurotoxin was detected after 2 weeks of incubation in samples at pH 5.4 or above, while it took 4 weeks for the toxin to be detected in samples at pH 5.2 to 5.3, and 12 weeks in samples at pH 5.0 to 5.1. In samples at pH 4.8 or below, no toxin was detected during the experimental period (24 weeks).

Type A toxin was detected in samples of pH $\geq$ 5.0. Type B toxin was detected only in samples of pH $\geq$ 5.4.

Uninoculated samples were not included in the neurotoxin assay as negative control because they were confirmed to be free of bacteria in aerobic and anaerobic counts.

DISCUSSION

When *C. botulinum* spores alone were inoculated into rice samples at a concentration of 2 log CFU/g, counts of this pathogen increased, and neurotoxin was detected in samples at initial pH 5.4 or above after 2 weeks of storage at 30°C. This result indicates that MAP-steamed rice products, which are usually at pH 6.5, are at risk of *C. botulinum*–toxin formation when secondary contamination with this organism occur. On the other hand, Kazama et al. *(9)* reported that at least 1 month was needed before the toxin could be detected in the same type of sample stored at 30°C, with much higher inoculation load (4.2 log CFU/g). The only difference between their experimental design and ours was the control of atmospheric conditions in the packaging. They used a deoxidant pack to decrease the O_2 content but did not pack the samples under a modified atmosphere. Their method might have allowed high initial and subsequent O_2 content in the package, as our previous experiments showed that the use of deoxidant pack alone is not sufficient to produce a completely anaerobic atmosphere (data not shown). In fact, our data show that a long incubation time (2 to 3 months) is required for *C. botulinum*–toxin production and growth in rice products stored at oxygen concentration of 0.4% (data not shown). Since Kazama et al. *(9)* did not indicate the oxygen concentration in their report, it is not known what O_2 content prevents the growth of *C. botulinum*. In contrast to their experiments, our experiments were based on the worst-case scenario, using oxygen concentration of $\leq$0.3%, since we think that risk assessment of any foodborne pathogen must be carried out based on the worst-case scenario.

In samples at pH 4.9 or below, anaerobic counts did not increase from the initial counts, and neurotoxin was not detected during the entire experimental period used in this study. It is well reported that toxin production is not limited above pH 4.6 in pure cultures of *C. botulinum* isolated from food contamination cases *(21)*. This inconsistency of pH threshold may be attributed to the unique properties of aseptically steamed rice samples. Rice is composed almost entirely of starch, with little protein *(18)*, and proteolytic *C. botulinum* has limited ability to utilize starch as a carbon source *(15)*, although under optimized conditions, at least some strains could utilize starch *(20)*, and high-starch foods such as potatoes could be the source of an outbreak *(1)*. Moreover, when *C. botulinum* and *Bacillus subtilis* were grown together on rice, *B. subtilis* was reported to promote the growth and toxin production of *C. botulinum (8)*, as amylase produced by *B. subtilis* digests starch that then stimulates the growth of *C. botulinum*. Other researchers have also reported that the presence of other microbial species allows *C. botulinum* to grow and produce neurotoxins *(6, 14)*. For example, the presence of molds results in increased *C. botulinum* growth and allows neurotoxin production at pH 4.2 *(7)*. This is possible because molds not only produce amylase, but also locally increase the pH *(7)*. In the present study, we inoculated *C. botulinum* alone into rice samples. Thus, the effects of co-inoculation with other microorganisms should be studied further. Also, since botulinum toxin type A was produced at pH 4.75 and water activity of 0.97 in vacuum-packed potatoes acidified with organic acid, other factors contributing to inhibition remain to be identified *(4)*.

Unexpectedly low anaerobic count corresponding with no toxin production was observed for samples at pH 5.2 to 5.3 collected at week 12 (Table 1). All three samples had similar anaerobic counts, and the pH values and atmospheric compositions were sufficient for *C. botulinum* to multiply and produce toxins. Therefore, the reason for these results is not known.

In conclusion, we demonstrated the worst-case scenario of botulism in steamed rice products after inoculation of *C. botulinum* spores alone under an atmosphere of $\leq$0.3% oxygen. We conclude that aseptically steamed rice products must be adjusted to pH 4.9 or below to avoid the risk of botulism from consumption of these MAP foods.

ACKNOWLEDGMENTS

The authors thank Y. Kasai (Laboratory of Food Microbiology, Tokyo University of Marine Science and Technology) for his technical instruction. The authors also acknowledge Dr. H. Nakano and the National Institute of Infectious Diseases for the kind gifts of proteolytic *C. botulinum* strains. This work was partly supported by the Food Safety Commission of Japan (0705), Japanese Ministry of Health, Labor and Welfare (H19-011), the National Food Research Institute of Japan (project: Development of evaluation and management methods for supply of safe, reliable and functional food and farm produce), and a Grant-in-Aid for Scientific Research (C 15580179) from the Ministry of Education, Science, Sports and Culture of Japan.

REFERENCES

1. Angulo, F. J., J. Getz, J. P. Taylor, K. A. Hendricks, C. L. Hatheway, S. S. Barth, H. M. Solomon, A. E. Larson, E. A. Johnson, L. N. Nickey, and A. A. Ries. 1998. A large outbreak of botulism: the hazardous baked potato. *J. Infect. Dis.* 178:172–177.
2. Bladel, B. O., and R. A. Greenberg. 1965. Pouch method for the isolation and enumeration of clostridia. *Appl. Microbiol.* 13:281–285.
3. Daifas, D. P., J. P. Smith, B. Blanchfield, and J. W. Austin. 1999. Effect of pH and CO_2 on growth and toxin production by *Clostrid-*

ium botulinum in English-style crumpets packaged under modified atmosphere. *J. Food Prot.* 62:1157–1161.
4. Dodds, K. L. 1989. Combined effect of water activity and pH on inhibition of toxin production by *Clostridium botulinum* in cooked, vacuum-packed potatoes. *Appl. Environ. Microbiol.* 55:656–660.
5. Fujisawa, T., K. Aikawa, I. Furukawa, and T. Takahashi. 2000. Occurrence of clostridia in glass bottled foods. *Int. J. Food Microbiol.* 54:213–221.
6. Hotchkiss, J. H., M. J. Banco, F. F. Busta, C. A. Genigeorgis, R. Kochiba, L. Rheaume, L. A. Smoot, J. D. Schuman, and H. Sugiyama. 1992. The relationship between botulinal toxin production and spoilage of fresh tomatoes held at 13 and 23°C under passively modified and controlled atmospheres and air. *J. Food Prot.* 55:522–527.
7. Huhtanen, C. N., J. Naghski, C. S. Custer, and R. W. Russell. 1976. Growth and toxin production by *Clostridium botulinum* in moldy tomato Juice. *Appl. Environ. Microbiol.* 32:711–715.
8. Kasai, Y., B. Kimura, S. Kawasaki, T. Fukaya, K. Sakuma, and T. Fuji. 2005. Growth and toxin production by *Clostridium botulinum* in steamed rice aseptically packed under modified atmosphere. *J. Food Prot.* 68:1005–1011.
9. Kazama, A., T. Muta, and N. Matsuda. 1994. Effects of pH on toxin production in hermetically packaged steamed rice by *Clostridium botulinum* types A and B and heat resistance of those spores. *Jpn. J. Food Microbiol.* 11:165–171.
10. Kimura, B., S. Kuroda, M. Murakami, and T. Fujii. 1996. Growth of *Clostridium perfringens* in fish fillets packaged with a controlled carbon dioxide atmosphere at abuse temperatures. *J. Food Prot.* 59: 704–710.
11. Koseki, S., and K. Itoh. 2002. Effect of nitrogen gas packaging on the quality and microbial growth of fresh-cut vegetables under low temperatures. *J. Food Prot.* 65:326–332.
12. Lambert, A. D., J. P. Smith, and K. L. Dodds. 1991. Effect of initial O_2 and CO_2 and low-dose irradiation on toxin production by *Clostridium botulinum* in MAP fresh pork. *J. Food Prot.* 54:939–944.
13. Lyver, A., J. P. Smith, J. Austin, and B. Blanchfield. 1998. Competitive inhibition of *Clostridium botulinum* type E by *Bacillus* species in a value-added seafood product packaged under a modified atmosphere. *Food Res. Int.* 31:311–319.
14. Odlaug, T. E., and I. J. Pflug. 1979. *Clostridium botulinum* growth and toxin production in tomato juice containing *Aspergillus gracilis*. *Appl. Environ. Microbiol.* 37:496–504.
15. Sneath, P. H. A., N. S. Mair, M. E. Sharpe, and J. G. Holt (ed.). 1986. Bergey's manual of systematic bacteriology, 8th ed. Williams & Wilkins, Baltimore, Md.
16. Solomon, H. M., E. J. Rhodehamel, and D. A. Kautter. 1998. Growth and toxin production by *Clostridium botulinum* on sliced raw potatoes in a modified atmosphere with and without sulfite. *J. Food Prot.* 61:126–128.
17. Torre, M. D., M. L. Stecchini, and M. W. Peck. 1998. Investigation of the ability of proteolytic *Clostridium botulinum* to multiply and produce toxin in fresh Italian pasta. *J. Food Prot.* 61:998–993.
18. U.S. Department of Health, Education, and Welfare. 1972. Food composition table for use in east Asia 1972. U.S. Department of Health, Education, and Welfare, Food and Agriculture Organization, Food Policy and Nutrition Division, Bethesda, Md.
19. U.S. Food and Drug Administration. 2001. Bacteriological analytical manual. AOAC International, Gaithersburg, Md.
20. Whitmer, M. E., and E. A. Johnson, 1987. Development of improved defined media for *Clostridium botulinum* serotypes A, B, and E. *Appl. Environ. Microbiol.* 54:753–759.
21. Wong, D. M., K. E. Young-Perkins, and R. L. Merson. 1988. Factors influencing *Clostridium botulinum* spore germination, outgrowth, and toxin formation in acidified media. *Appl. Environ. Microbiol.* 54:1446–1450.

Journal of Food Protection, Vol. 71, No. 4, 2008, Pages 839–844

Research Note

Use of Single-Strand Conformation Polymorphism of Amplified 16S rDNA for Grouping of Bacteria Isolated from Foods

HAJIME TAKAHASHI,[1] BON KIMURA,[1]* YUICHIRO TANAKA,[1,2] MAYUMI MORI,[1] ASAMI YOKOI,[1] AND TATEO FUJII[1]

[1]*Department of Food Science and Technology, Faculty of Marine Science, Tokyo University of Marine Science and Technology, 4-5-7, Konan, Minato, Tokyo 108-8477, Japan; and* [2]*Department of Quality Assurance, Toyo Suisan Kaisha, Ltd., Tokyo 108-8501, Japan*

MS 07-498: Received 17 September 2007/Accepted 14 December 2007

ABSTRACT

The grouping method for isolated strains from foods using single-strand conformation polymorphism (SSCP) after PCR amplification of a portion of 16S rDNA was developed. This method was able to group the strains from various food samples based on 16S rDNA sequence. As 97.8% of the isolated strains from various foods were grouped correctly, use of the PCR-SSCP method enables the prompt and labor-saving analysis of microbial population of food-derived bacterial strains. Advantages in speed and accuracy of bacterial population identification by the PCR-SSCP method have practical application for food suppliers and testing laboratories.

For food manufacturers, aerobic plate count (APC) is widely used as a standard method for microbiological quality control. Although the importance of the APC remains unchanged, the demand for identification techniques of bacterial species is increasing to obtain the detailed information about APC result. An abnormal APC, a result that deviated from specification(s) formulated by public administration or the food industry, requires further analysis in order to identify isolates to analyze the microbial population.

Denaturing gradient gel electrophoresis (DGGE) *(16)*, one of the electrophoretic typing methods of DNA, is widely used to analyze microbial communities in combination with DNA sequencing of the separated DNA fragments *(6, 10, 21–23)*. DGGE is a useful method for rapid and comparative analysis of complex bacterial flora. However, as the DGGE method uses DNA extracted directly from the sample and amplified by PCR, comparative analysis with APC is difficult because the nonculturable bacteria on the APC plate are also detected by DGGE. In addition, the quantitative differences of bacterial species in a sample are not clearly identified by the DGGE method. The microbial population analysis by the food manufacturers is generally carried out by identifying 10 to 20 of the randomly isolated strains from the countable APC plates. Analysis of microbial populations by this conventional method enables the semiquantitative comparison of the constituents. However, identification of 10 to 20 of the bacterial isolates is both a time- and labor-intensive process.

The strategy of selecting representative strains from isolated strains following DNA typing is an easy and simple way to decrease the identification operation. The PCR–restriction fragment length polymorphism (RFLP) method is frequently used for this purpose. We consider that the PCR-RFLP targeting 16S rDNA is a simple and useful technique; however, it is limited in terms of analyzing bacterial populations promptly. The technique is time-consuming in terms of restriction enzyme processing, and the resolution is not sufficient. DGGE, temperature gradient gel electrophoresis, and single-strand conformation polymorphism (SSCP) are widely used for microbial community analysis. The SSCP method can recognize a single polymorphism in a DNA fragment *(19)*, and recently, this method has been applied to microbial community analysis *(9, 15, 20)*, including the identification of specific species *(25, 28)*. SSCP electrophoresis separates the single-stranded DNA not only according to its base length, but also according to the secondary structures of DNA. The secondary structure of DNA is affected by its sequence. We consider that SSCP is highly advantageous for grouping many strains in terms of rapidness and resolution. In this study, we evaluated a strategy based on the PCR-SSCP method for analyzing the microbial populations found in food products. We tested the accuracy of this grouping method in the samples of fresh fish products, meat, and vegetables.

MATERIALS AND METHODS

Bacterial isolation. Foods purchased from retail food shops in Tokyo and comprising three samples each of fish, meat, and vegetables were transported to the laboratory on ice. Twenty-five grams of each sample was homogenized with 225 ml of 0.85% NaCl saline, using a stomacher (Seward Co., Ltd., London, UK) for 1 min. Serial 10-fold dilutions (10^{-1} to 10^{-6}) were prepared, and 100 μl from each was plated in duplicate onto modified tryptic soy agar (Difco, Becton Dickinson, Sparks, Md.) supplemented with 1% NaCl and incubated at 30°C for 24 h. Colonies were counted, and 20 colonies from each sample type were randomly isolated from countable plates, without considering the appearance of colonies, and identified using the method below.

* Author for correspondence. Tel/Fax: 81-3-5463-0603; E-mail: kimubo@kaiyodai.ac.jp.

TABLE 1. *The result of PCR-SSCP analysis and identification results of 16S rDNA sequencing of food isolates*

Sample	Bacterial counts (CFU/g)	No. of groups of isolated strains by PCR-SSCP	Confirmation of PCR-SSCP grouping by 16S rDNA sequencing[a]			
			SSCP group	Closest relatives of 16S rDNA sequence (accession no. of closest relative)[b]	% similarity	No. of strains
Horse mackerel	4.3×10^3	9	1A	*Pseudoalteromonas elyakovii* (AF082562)	98	7
			1B	*Psychrobacter glacincola* (U85877)	98	6
			1C	*Arthrobacter globiformis* (AB098573)	94	1
			1D	*Brochothrix thermosphacta* (AY543029)	98	1
			1E	*Flavobacterium frigidarium* (AY771722)	99	1
			1F	*Photobacterium angustum* (D25307)	96	1
			1G	*P. phosphoreum* (AY780009)	98	1
			1H	*Pseudomonas tolaasii* (EF111117)	97	1
			1I	*Vibrio rumoiensis* (DQ530292)	98	1
Tuna	1.0×10^4	9	2A	*Acinetobacter johnsonii* (X81663)	97	7
			2B[c]	*Chryseobacterium/Flavobacterium*	—	2
			2C	*Acinetobacter haemolyticus* (X81662)	98	3
			2D	*Psychrobacter glacincola* (U85878)	99	2
			2E	*Stenotrophomonas maltophilia* (AY367030)	97	2
			2F	*Arthrobacter bergeri* (AJ609633)	99	1
			2G	*Pseudomonas fluorescens* (AY512614)	97	1
			2H	*P. lurida* (AJ581999)	98	1
			2I	*Sphingobacterium spiritivorum* (EF090267)	92	1
Young yellowtail	1.2×10^3	6	3A	*Shewanella frigidimarina* (U85902)	99	7
			3B	*A. johnsonii* (DQ911549)	98	4
			3C	*Acinetobacter lwoffi* (U10875)	89	2
			3D	*P. fluorescens* (DQ084459)	99	3
			3E	*Chryseobacterium benhlgensis* (EF154516)	97	3
			3F	*Pseudomonas putida* (EF690402)	99	1
Pork	8.1×10^3	11	4A	*Carnobacterium maltaromaticum* (AF270798)	99	5
			4B	*A. johnsonii* (EF204268)	98	4
			4C	*P. putida* (AY456706)	99	2
			4D	*Staphylococcus* spp.	99	2
			4E	*Acinetobacter baumannii* (X81667)	96	1
			4F	*Aeromonas hydrophila* (AY264937)	100	1
			4G	*Carnobacterium maltaromaticum* (AF184247)	98	1
			4H	*Chryseobacterium soldanellicola* (AY883415)	96	1
			4I	*Enterobacter agglomerans* (AF157694)	97	1
			4J	*Pseudomonas migulae* (AF074383)	99	1
			4K	*Staphylococcus* spp.	99	1
Chicken	5.2×10^4	12	5A	*Pseudomonas libanensis* (DQ288882)	99	7
			5B	*A. hydrophila* (X87271)	98	3
			5C	*Acinetobacter junii* (EF429000)	99	1
			5D	*Brochothrix thermosphacta* (AY543017)	99	1
			5E	*Carnobacterium divergens* (AY543016)	99	1
			5F	*Chryseobacterium indoltheticum* (M58774)	97	1
			5G	*P. fluorescens* (AF228367)	98	1
			5H	*P. fluorescens* (DQ178230)	99	1
			5I	*Pseudomonas meridiana* (AJ537602)	99	1
			5J	*P. fragi* (D84014)	98	1
			5K	*P. migulae* (AY047218)	97	1
			5L	*P. fluorescens* (DQ178232)	99	1
Beef	8.8×10^5	3	6A	*Carnobacterium maltaromaticum* (AY543018)	99	18
			6B	*Moraxella osloensis* (Y15855)	99	1
			6C	*Staphylococcus* spp.	99	1
Daikon radish sprout	2.0×10^8	9	7A	*Stenotrophomonas maltophilia* (AJ293473)	99	8
			7B	*S. rhizophia* (AJ293463)	97	3
			7C	*S. maltophilia* (AB021406)	99	3
			7D	*Chryseobacterium piscium* (AM040439)	99	1
			7E	*Comamonas testosteroni* (AF519533)	99	1
			7F	*A. johnsonii* (AB099655)	99	1
			7G	*Pseudomonas fulgida* (AJ492830)	99	1
			7H	*P. putida* (AY647158)	98	1
			7I	*Sphingobacterium multivorum* (AB100738)	99	1

TABLE 1. *Continued*

Sample	Bacterial counts (CFU/g)	No. of groups of isolated strains by PCR-SSCP	Confirmation of PCR-SSCP grouping by 16S rDNA sequencing[a]			
			SSCP group	Closest relatives of 16S rDNA sequence (accession no. of closest relative)[b]	% similarity	No. of strains
Lettuce	5.6×10^7	7	8A	*Pseudomonas cichorii* (AB021398)	99	11
			8B[d]	*Enterobacter/Erwinia*	—	3
			8C	*P. putida* (AY456706)	99	2
			8D	*Chryseobacterium formosense* (AY315443)	98	1
			8E	*Pseudomonas veronii* (AB056120)	99	1
			8F	*P. marginalis* (Z76663)	99	1
			8G	*P. borealis* (AJ012712)	99	1
Bean sprout	2.2×10^7	7	9A[e]	*Enterobacter/Erwinia/Raoultella*	—	11
			9B	*Pseudomonas* spp.	98	4
			9C	*P. oryzihabitans* (AM262973)	98	1
			9D	*E. agglomerans* (AF130961)	96	1
			9E	*E. amnigenus* (EF426859)	98	1
			9F	*E. asburiae* (EF059885)	99	1
			9G	*P. oryzihabitans* (AY850170)	99	1

[a] Isolated strains from each food samples were grouped by PCR-SSCP, and all strains were identified by 16S rDNA sequencing.
[b] Identification by 16S rDNA sequencing was performed using an approximately 500-bp portion of 16S rDNA (*E. coli* position 50 to 500). After the database was searched, strains were identified as the closest relatives.
[c] Group 2B consisted of two species: two strains of *C. piscium* (DQ862541, 97%) and a strain of *Flavobacterium denitrificans* (AJ308927, 95%).
[d] Group 8B consisted of two species: two strains of *E. agglomerans* (Z96083, 99%) and *Erwinia persicina* (AM184098, 97%).
[e] Group 9A consisted of three species: nine strains of *E. agglomerans* (AF130939, 98%), *Erwinia rhapontici* (AJ233417, 100%), and *Raoultella planticola* (Y17663, 97%).

Identification of isolated strains by 16S rDNA sequencing. Samples of DNA for PCR templates were extracted based on chaotropic extraction, followed by absorption onto silica-coated magnetic beads using a commercially available DNA extraction kit (Mag Extractor-Genome, Toyobo Co., Ltd., Tokyo, Japan) according to manufacturer's instructions. Briefly, 1 ml of the overnight culture of each isolated strain in tryptic soy broth (Difco, Becton Dickinson) supplemented with 1% NaCl was centrifuged (15,000 × *g*, 5 min), resuspended in 850 μl of lysis buffer, applied to 40 μl of silica-coated magnetic beads, and vortexed vigorously for 10 min. The magnetic beads were then precipitated by tabletop centrifugation (2,000 × *g*, 15 s), washed twice in 900 μl of washing buffer and once in 900 μl of 70% ethanol, and finally resuspended in 100 μl of Tris-EDTA buffer. After the suspension was vortexed vigorously for 10 min, the magnetic beads were precipitated by tabletop centrifugation (2,000 × *g*, 15 s), and the supernatant was collected for use in PCR reactions.

All strains were identified by amplifying and sequencing an approximately 450- to 500-bp portion of 16S rDNA (*Escherichia coli* positions 50 to between 450 and 500) *(2)*. Amplification was performed using universal primers 27F and 1492R *(27)*, and products were purified by ultrafiltration (Montage PCR centrifugal filter devices, Millipore Corp., Bedford, Mass.). Purified products were then directly sequenced using Texas Red–labeled primers 27F and 536R *(27)* by the DNA sequencer SQ5500E (Hitachi, Ltd., Tokyo, Japan) with the Thermo Sequenase primer cycle sequencing kit (GE Healthcare UK, Ltd., Amersham Place, Little Chalfont, Buckinghamshire, UK). The BLAST 2.0 algorithm was used to compare the derived sequences with 16S rDNA sequences in the DDBJ database (http://www.ddbj.nig.ac.jp, Shizuoka, Japan).

SSCP analysis of 16S rDNA V3 region. In the PCR-SSCP analysis, we used precast polyacrylamide gel, followed by silver staining because of the high sensitivity of silver staining. This method visualizes even a small amount of nonspecific amplification product; therefore, several PCR primers and thermal profiles were tested for specificity and the difference of PCR efficiency. The primer set SRV3-1 (5′-CGG YCC AGA CTC CTA CGG G-3′) *(15)* for forward primer and V3R53 (5′-GTA TTA CCG CGG CTG CTG GC-3′), which was newly designed based on 536R *(27)* with minor modifications for reverse primer, gave acceptable results. PCR amplification was performed in 100-μl reaction mixtures composed of 10 mM Tris-HCl (pH 8.3), 50 mM KCl, 1.5 mM $MgCl_2$, 50 pmol each of primer, 0.2 mM each of four dNTPs, 2.5 U of TaKaRa *Taq* DNA polymerase (Takara Bio, Shiga, Japan), and 50 ng of template DNA. To minimize amplification of nonspecific products, touchdown PCR *(7)* was performed; the initial annealing temperature was set at 6°C above the target annealing temperature and decreased by 0.6°C every second cycle until the target annealing temperature, 61°C, was reached, and then 5 additional cycles were carried out with the target annealing temperature. Amplifications were carried out in a GeneAmp 9700 thermal cycler (Applied Biosystems, Foster City, Calif.), using the following cycle: denaturation at 94°C for 30 s, annealing at the temperature regime described above for 30 s, and primer extension at 72°C for 10 s for touchdown cycles, and 72°C for 30 s for the last 5 additional cycles.

SSCP analysis of PCR products was performed as described previously *(23)*. Briefly, PCR products were mixed 1:2 with loading buffer (98% formamide–10 mM EDTA–0.5% bromophenol blue), denatured by heating for 10 min at 100°C, cooled on ice, loaded in a precast, ready-to-use gel (GeneGel Excel 12.5/24 kit, GE Healthcare), and electrophoresed on a GenePhor electrophoresis unit (GE Healthcare) at 650 V, 25 mA, and 15°C until the bromophenol blue front reached the anode buffer strip (about 90 min). The gel was stained with a PlusOne DNA silver staining kit (GE Healthcare). Scanned photographs of SSCP gels were stored as TIFF images.

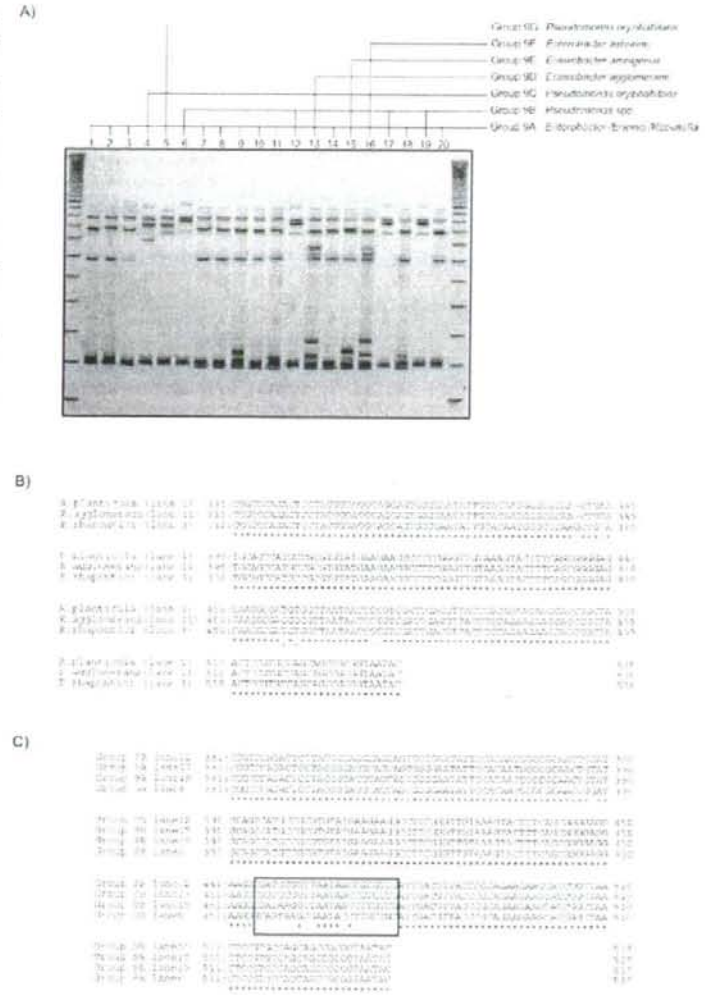

FIGURE 1. *Representative SSCP analysis results of the V3 region PCR product (bean sprout isolates). (A) Lanes: 1–3, 7–11, 14, 18, and 20 are group 9A; lanes 6, 12, 17 and 19 are group 9B; and lanes 4, 13, 15, 16, and 5 are group 9C to 9G, as shown in Table 1. The 100-bp DNA size marker was loaded on both sides, without heat denaturation. The bands that correspond to approximately 200 bp were double-stranded DNA. (B) Representative sequence alignment of the V3 region of group 9A strains. The fragments generated from these three genera were not separated by the PCR-SSCP method because of the high sequence similarity. (C) Sequence alignment of the V3 region of group 9B strains. The SSCP electrophoresis could not discriminate the polymorphisms indicated by the box, as described in the text.*

RESULTS AND DISCUSSION

Optimization of SSCP analysis. We selected the V3 region of 16S rDNA as the amplification target of the PCR-SSCP analysis because the V3 region of 16S rDNA is informative in the differentiation of bacterial strains. Nine of the V (hypervariable) regions, which contain many polymorphisms among species, are present in bacterial 16S rDNA *(18)*, and some are useful for bacterial classification alone or in combinations of two or more regions *(3)*. The V3 region is the third V region from the 5′ end of 16S rDNA and is positioned at 330 to 530 by *E. coli* numbering *(14)* and is widely used for typing or sequence identification of bacteria *(12, 29)*.

Amplification was performed using the touchdown PCR method *(7)*, in order to minimize nonspecific amplification products. In 80 strains (60 isolated strains from fresh fish products and 20 isolated strains from chicken; Table 1), the primer pair and the touchdown PCR conditions produced sufficient amounts of amplification products, with no undesired products (data not shown). The electrophoresis temperatures were also optimized for optimal separation of the 16S rDNA V3 fragment, and the optimal running temperature was determined to be 15°C. Theoretically, denaturation of a double-stranded DNA fragment provides two single-stranded DNA with different sequences. For this reason, two bands should be observed in PCR-SSCP analysis. However, some samples produced three or four bands by the PCR-SSCP method used here (Fig. 1; e.g., lanes 13 and 16). This occurred due to the high resolution of the PCR-SSCP method, which can detect substitutions of just a few bases. These results had no effect on the groupings since the banding was due to the heterogeneity among multiple copies of 16S rDNA *(4, 11, 17, 20)*.

Evaluation of the accuracy of SSCP analysis. We isolated 180 bacterial strains from nine food samples of fresh fish products, meat, and vegetables. All isolated strains were typed by the PCR-SSCP method (Fig. 1, representative result of bean sprout isolates), and then all strains were identified by 16S rDNA sequencing to confirm the grouping by PCR-SSCP. The 180 strains isolated in our study (20 strains each from nine food samples) were analyzed by PCR-SSCP, and 20 isolates from each food sample category were classified into 3 (beef) to 12 (chicken) groups (Table 1). Groupings by PCR-SSCP and 16S rDNA sequencing showed good correlation to the genus level (Table 1). For example, the groupings based on PCR-SSCP analysis of beef samples showed perfect correspondence to those of 16S rDNA sequencing analysis (Table 1). The perfect correspondences of grouping by PCR-SSCP analysis to 16S rDNA sequence were obtained for the other samples except tuna, lettuce, and bean sprouts as discussed below. These results indicate that PCR-SSCP is useful for grouping strains isolated from food samples. There is not a large influence in microbial population analysis results, although some of the isolates from tuna, lettuce, and bean sprout samples were not grouped perfectly.

Undesirable discrimination patterns of PCR-SSCP would be the grouping together in the same SSCP group of different strains belonging to different genera. Such imperfect grouping leads to the overlooking of the constituent bacteria in the sample. In this study, it was difficult to categorize some strains into the correct group. As shown in Table 1, two strains of *Chryseobacterium* and one strain of *Flavobacterium* from tuna fillets were grouped together. In isolates from lettuce, two strains of *Enterobacter* and a strain of *Erwinia* were grouped together (Table 1). In isolates from bean sprouts, nine strains of *Enterobacter,* one strain of *Raoultella,* and one strain of *Erwinia* were grouped together (Table 1 and Fig. 1A). When minority strains in a group for which two genera were observed, PCR-SSCP, as performed in this study, misidentified these 4 strains (2.2%) among a total of 180 strains. These inconsistencies were caused by the close genetic relationships among these strains. In fact, *Chryseobacterium* and *Flavobacterium* (isolates of both were found in tuna fillets) had been formally classified as the same genus *Flavobacterium (26). Enterobacter* and *Raoultella* (formally classified in *Klebsiella, (8)*) found in lettuce and bean sprouts could not be discriminated by 16S rDNA sequencing because they have sequence differences of only a few bases in the V3 region of their 16S rDNA (Fig. 1B). Also, the 16S rDNA sequence of *Erwinia* spp. found in bean sprouts was very similar to that of *Raoultella* in a DNA database search (98.5%). The results in our study indicate that substitutions of at least five bases in the V3 region of the 16S rDNA (2.5% difference) were reflected in the banding patterns of PCR-SSCP, except the substitutions at a specific position (*E. coli* position 457 to 480; Fig. 1C). The region 457 to 480 contains stem-loop structure of the 16S rRNA, and some of the base changes occurring at the loop area would not influence the secondary structure of the 16S rRNA. Since the banding patterns of SSCP electrophoresis reflect the single-strand conformation of the DNA, mutations at the position 457 to 480 are not always reflected in the PCR-SSCP banding patterns. This insufficiency did not lead the isolated strains belonging to the different genus into the same SSCP group, and only observed in SSCP group 9B of bean sprout sample used in this study. In general, molecular identification using 16S rDNA is a powerful tool in bacterial identification. However, it is not always sufficient for identification to the species level among groups containing genetically diverged species (*Bacillus* group) *(1),* genetically closed species (*Staphylococcus* group) *(24),* or ambiguously defined species (*Clostridium* group) *(5, 13).* These cases indicate the resolution limitations of the method using the V3 region of 16S rDNA. It is remarkable that our PCR-SSCP method did not fail to discriminate distant genera and clearly reflected the results of 16S rDNA sequencing.

In this study, nine food samples were tested and the 20 isolates from each food sample category were grouped into 3 to 12 (average of 8) groups by the PCR-SSCP method, and the same isolates were grouped into 3 to 8 (average of 6) genera by 16S rDNA sequencing (Table 1). Although the PCR-SSCP method occasionally grouped the same species into different groups (Table 1, SSCP group 4A and 4C, 5G and 5H, 7A and 7C, 9C and 9G), this did little to influence the accuracy of the analysis. Cost of analysis is increased because sequencing is carried out for the strains grouped together where it is not necessary. These problems occur due to the high resolution of this method, which can discriminate even a few bases of mutation.

We also analyzed the similarities of PCR-SSCP banding patterns and 16S rDNA sequences between the isolated strains using band imaging software (BioNumerics, Applied Maths BVBA, Kortrijk, Belgium), which identifies the strains by banding patterns. There were no correlations observed between the similarities of SSCP banding patterns and 16S rDNA sequences, because SSCP banding patterns are not directly affected by sequence substitutions, but rather by differences in secondary structure of the single-strand DNA caused by sequence substitution *(15).* The SSCP banding pattern database may be provided in future experiments for the strain identification by only using this PCR-SSCP method.

The analyses carried out in this study required a total of 4 days. On the first day, we plated food samples onto medium; on the second day, colonies were counted and were picked. On the third day, chromosomal DNA of isolated strains were extracted using the commercially available kit, the V3 regions of 16S rDNA were amplified, and the DNA samples were applied to SSCP analysis and the representative strains selected from each SSCP group. The 16S rDNA sequences of the representatives were determined and strains were identified on the fourth day. Since precast gels and all reagents are commercially available as a ready-to-use package, the PCR-SSCP method has excellent reproducibility among experiments and technicians. Moreover, the multiprocessor (GE Healthcare) is now available and makes technician-free operation possible for the staining step. The total cost to analyze 20 isolates (one food